

DESIGN AND ANALYSIS OF FRACTAL ANTENNA FOR UWB COMMUNICATION AND BIOMEDICAL APPLICATIONS

A Project Dissertation submitted in partial fulfillment of the
requirements for the degree of

MASTER OF TECHNOLOGY IN MICROWAVE AND OPTICAL COMMUNICATION

Submitted by:

NANCY (2K20/MOC/04)

Under the supervision of:

Mr. Kaustubh Ranjan Singh



**ELECTRONICS & COMMUNICATION
DELHI TECHNOLOGICAL UNIVERSITY**
(Formerly Delhi College of Engineering)

Bawana Road, Delhi-110042

MAY 2022

CANDIDATE'S DECLARATION

I, Nancy (2K20/MOC/04), student of M. Tech, Microwave and Optical Communication, hereby declare that the major project dissertation titled “**DESIGN AND ANALYSIS OF FRACTAL ANTENNA FOR UWB COMMUNICATION AND BIOMEDICAL APPLICATIONS**” which is submitted by me to the Department of Electronics and Communication Engineering, Delhi Technological University, Delhi in partial fulfillment of the requirement for the award of the degree of Master of Technology, is original and not plagiarized from any source without proper citation. This work has not previously formed the basis for the award of any Degree, Diploma, Associateship, Fellowship, or any other similar title or recognition.

Place: **New Delhi**

Date: May 31, **2022**

NANCY(2K20/MOC/04)

**ELECTRONICS & COMMUNICATION
DELHI TECHNOLOGICAL UNIVERSITY**

(Formerly Delhi College of Engineering)

Bawana Road, Delhi-110042

MAY 2022

CERTIFICATE

I hereby certify that the Project Dissertation titled “**DESIGN AND ANALYSIS OF FRACTAL ANTENNA FOR UWB COMMUNICATION AND BIOMEDICAL APPLICATIONS**” which is submitted by Nancy (2K20/MOC/04), to the department of Electronics and Communication Engineering, Delhi Technological University, Delhi in partial fulfillment of the requirement for the award of the degree of Master of Technology during session 2020-2022, is a record of the major project work carried out by the student under my supervision. To the best of my knowledge this work has not been submitted in part or full for any Degree or Diploma to this University or elsewhere.



Mr. Kaustubh Ranjan Singh

SUPERVISOR

**ELECTRONICS & COMMUNICATION
DELHI TECHNOLOGICAL UNIVERSITY
(Formerly Delhi College of Engineering)
Bawana Road, Delhi-110042
MAY 2022**

ACKNOWLEDGEMENT

The success and final outcome of this project required a lot of guidance and assistance from many people, and I am extremely fortunate to have got this all along the completion of my project work. Hence, it is only befitting that I thank them all. First and foremost, I would like to express my gratitude to my mentor, Mr. Kaustubh Ranjan Singh, Department of Electronics and Communication Engineering, Delhi Technological University for his constant support and guidance which helped me complete the project on time. He has always been a source of inspiration, and has always been there for me in all our times of need. He is extremely amicable and approachable, and makes working in any project enjoyable, and enriching. It was an absolute pleasure working under his able guidance.

Our thanks go to my family and friends for always being there in times of distress, and for their untiring support.

Lastly, we would like to thank God almighty for ensuring no unforeseen obstacles stayed for long during the course of our work.

NANCY

ABSTRACT

Various characteristics of fractals have been used in making antennas for a very long time. Fractal geometries have made it possible to use a single antenna for various applications due to its wideband and multiband property, as it maximizes the effective length of the antenna without any use of inductors or capacitors.

Multiband Fractal antenna designs have been proposed in this thesis. Analysis of fractal antenna was done by using the software named Ansys HFSS 15.0. Antenna simulated showed multiband characteristics with compact, light-weight, and easy to fabricate the design. The first antenna is based on Sierpinski Gasket geometry. It operates in a multiband frequency range of 4.1- 10.9 GHz and 20.7-33.4 GHz. The second antenna is based on Sierpinski Carpet geometry. It operates in a multiband frequency range of 5.2-6.4 GHz, 7.6-11.3 GHz, and 19-30.9 GHz. The third antenna is based on Koch curve geometry. It operates in a multiband frequency range of 4.6- 11.1 GHz and 20.8-28.1 GHz.

Biomedical implantable antenna using fractals have been designed which requires properties like compact size, low specific absorption rate, flexibility, and wideband characteristics. For proper positioning of the antenna inside the human body, the size of the antenna must be small. Various techniques are used for the miniaturization of the antenna, including concentric ring slots in the shape of a rectangle. Flexibility is another requirement for the implantable antenna. This prevents the breakage of the antenna with any movement of the body part of the muscle. Thin and flexible layers of substrate and superstrate are used to provide flexibility. Also, these layers should be biocompatible. The antenna is covered with a thin layer of biocompatible material to enhance its performance by reducing the absorption in the lossy environment. A reduced antenna gain has been observed due to the absorbing nature of the human body. So, to improve the antenna gain, different techniques are used, namely external parasitic ring and hemispherical lens along with the encapsulation layer around the antenna.

CONTENTS

Candidate’s Declaration -----	i
Certificate -----	ii
Acknowledgement -----	iii
Abstract -----	iv
Contents	
List of Figures -----	ix
List of Tables -----	x
CHAPTER 1 Thesis Overview	1
1.1 Introduction	2
1.2 Literature Review	4
1.3 Chapter Outline	5
1.4 Summary	6
CHAPTER 2 Fractal Antenna	7
2.1 Introduction	8
2.2 Fractal Theory	8
2.3 Fractal Geometries	11
2.4 Fractal Antenna	13
CHAPTER 3 Antenna based on different Fractal Geometries	16
3.1 Fractal antenna based on Sierpinski Carpet geometry	17
3.1.1 Introduction	17
3.1.2 Antenna Design	17

3.1.3 Simulation Results	19
3.1.4 Summary	23
3.2 Fractal antenna based on Sierpinski Gasket geometry	24
3.2.1 Introduction	24
3.2.2 Antenna Design	24
3.2.3 Simulation Results	25
3.2.4 Summary	29
3.3 Fractal antenna based on Koch Curve geometry	30
3.3.1 Introduction	30
3.3.2 Antenna Design	30
3.3.3 Simulation Results	31
3.3.4 Summary	35
CHAPTER 4 Biomedical implantable antenna using fractal geometry	36
4.1 Introduction	37
4.2 Antenna Design	49
4.3 Simulation Results I	41
4.4 Placement of implantable antenna	44
4.4.1 Inside the muscle-layer model	44
4.4.2 Two-layer and three-layer model	45
4.5 Simulation Results II	45
4.6 Summary	46
CHAPTER 5 Gain enhancement of biomedical implantable antenna	49

5.1 Introduction	50
5.2 Gain enhancement techniques	51
5.3 Simulation Results	54
5.4 Summary	58
CHAPTER 6 Conclusion and Future Work	59
6.1 Conclusion	60
6.2 Future Work	62
CHAPTER 7 References	63
CHAPTER 8 Publication Details	65

LIST OF FIGURES

1.1 Applications of biomedical implantable antenna	3
2.1 Mandelbrot Set	9
2.2 Types of Fractals	10
2.3 Sierpinski Gasket Geometry	11
2.4 Sierpinski Carpet Geometry	12
2.5 Koch Curve Geometry	13
3.1.1 Antenna Design Fractal Antenna based on SierpinskiCarpet Geometry	18
3.1.2 Return Loss Plot	18
3.1.3 Geometry of the proposed antenna	19
3.1.4 Return Loss Plot	20
3.1.5 VSWR Plot	21
3.1.6 3-Dimenaionl Polar Plot	21
3.1.7 Radiation Pattern (E-Field)	22
3.1.8 Radiation Pattern (H-Field)	23
3.2.1 Antenna Design Fractal Antenna based on Sierpinski Carpet Geometry	25
3.2.2 Return Loss Plot (1 st , 2 nd and 3 rd iterations)	26
3.2.3 Return Loss Plot (4 th iteration)	26
3.2.4 VSWR Plot	27
3.2.5 3-Dimensional Polar Plot	27
3.2.6 Radiation Pattern (E-Field)	28
3.2.7 Radiation Pattern (H-Field)	29
3.3.1Antenna Design Fractal Antenna based on Koch Curve Geometry	31
3.3.2 Return Loss Plot (1 st and 2 nd iterations)	32
3.3.3Return Loss Plot (3 rd iteration)	32
3.3.4 VSWR Plot	33

3.3.5 3-Dimensional Polar Plot	33
3.3.6 Radiation Pattern (E-Field)	34
3.3.7 Radiation Pattern (H-Field)	35
4.1 Wireless Communication of Implantable Antenna System	37
4.2 Parts of Implantable medical devices	38
4.3 Geometry of proposed antenna. (0th iteration)	39
4.4 Geometry of proposed antenna. (1 st iteration, 2 nd iteration, 3 rd iteration)	41
4.5 Return loss plot (1st iteration, 2nd iteration)	42
4.6 Return loss plot (3rd iteration)	42
4.7 VSWR Plot (3rd iteration)	43
4.8 3-Dimensional polar plot and SAR plot	43
4.9 Radiation pattern (E-field and H-field)	44
4.10 2-layer and 3-layer model	45
4.11 Return loss plot (depths of muscle layer)	46
4.12 Return loss plot (different models)	46
5.1 Encapsulation layer around the implantable antenna	52
5.2 External Parasitic ring structure	52
5.3 External Parasitic lens structure	53
5.4 3-Dimensional polar plot (gain enhancement techniques)	54
5.5 Implantable antenna with external parasitic ring and lens.	55
5.6 Return loss plot	55
5.7 Return loss plot (all the techniques combined)	56
5.8 SAR (Specific absorption rate) plot	56
5.9 Radiation pattern (E-field and H-field)	57

LIST OF TABLES

1.1 Frequency bands allotted by FCC for biomedical implantable devices	4
2.1 Properties of Fractals and their utilization in making Fractal Antenna	14
3.1.1 Total Gain of various iterations	17
3.1.2 Parametric values of the proposed Fractal Antenna	20
3.1.3 Comparison of different iterations on the basis of gain and fractional bandwidth	24
3.2.1 Comparison of different iterations on the basis of gain and fractional bandwidth	30
3.3.1 Comparison of different iterations on the basis of gain and fractional bandwidth	35
4.1 Design parameters of the implantable antenna	40
4.2 Design parameters of the proposed fractal antenna	41
4.3 Comparison of different iterations on the basis of various parameters	47
4.4 Various Antenna parameters when the antenna is placed at various depths of muscle layer	47
4.5 Various Antenna parameters when the antenna is placed in different layers models	48
5.1 Optimizing radius and width of the ring	53
5.2 Optimizing radius of the lens of the implantable antenna	54
6.1 Comparison between different structures with different parameters	60
6.2 Comparison of different antenna models proposed in this thesis for improved gain	61

CHAPTER-1

THESIS OVERVIEW

1.1 INTRODUCTION

In today's modern world, the wireless communication industry has shown progress and growth following the initiation of the internet and cell phones. And thus, a need for more and more frequency bands. These devices also require small, compatible, affordable antennas and operate for more than one operating frequency band while maintaining their performance. To overcome these challenges, a new scheme of multi-band antennas is proposed.

Multiband antennas have various applications in modern wireless communication systems in which the downward and the roaming capability among multi-standards are demanded. The global system for mobile communication (GSM), the general packet radio service (GPRS), the wireless local area networks (WLAN), the universal mobile telecommunications system (UMTS), etc., are generally dual-band or multi-band wireless standards communication devices. So, both the requirement of the compact and multi-band antenna is fulfilled by fractal antennas. These antennas utilize fractal geometry concepts that are the self-similar patterns to maximize the antenna's effective length, which makes the antenna multi-band, wideband, and miniaturized without any use of inductors or capacitors. They are also known as space-filling curves as we can increase the perimeter while keeping its area constant. Many different fractal geometries like Sierpinski gasket, Sierpinski carpet, Koch curve, Minkowski island, etc., are used, which first involves a basic shape repeated repeatedly with every iteration it a multi-band antenna.

One of the major applications of a fractal antenna is implantable medical devices. From the diagnosis of a disease to its monitoring and treatment, these wireless devices are being used in modern medicine to improve the quality of the healthcare system that is cost-effective and less invasive. From pacemakers introduced in the 1960s to cancer detectors and endoscopy capsules with sensors, wireless IMDs play an essential role in providing data in real-time. Diseases like Hyperthermia, Diabetes detection, Heart stroke prevention, and some digestive disorders like inflammatory bowels, ulcerative colitis, etc., can be detected.

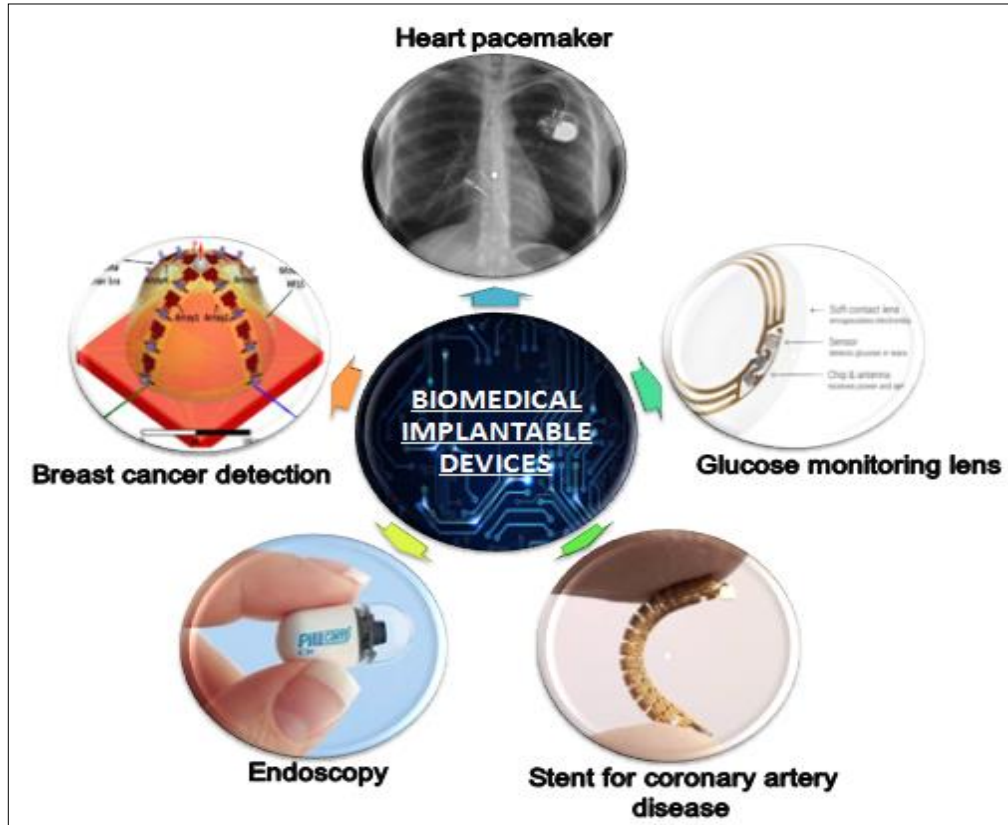


Figure.1.1 : Applications of biomedical implantable antenna

Biomedical devices like stents, pacemakers, capsules, pressure, temperature and glucose sensors, etc. Some of the devices are shown in the figure.1

These implantable devices consist of many components: Antenna, Sensors, Processors, batteries, and Storage devices. Wireless communication between implanted and external devices needs to be reliable and robust, which depends on the performance of the implantable antenna. This antenna is responsible for the transmission and reception of signals. For a compact size of the implanted device, the antenna should be lightweight and small. Nevertheless, antenna design becomes complex due to the lossy environment of the human body.

Federal Communication Commission (FCC) has allotted frequency bands for medical implant services as given in Table.1

S. No.	Bands	Frequency allotted
1	MICS (Medical implant communications service)	402-405 MHz
2	ISM (Industrial, scientific and medical)	2.45 GHz
3	MedRad (Medical device radio band)	401-406, 413-419, 426-432, 438-444, 451-457 MHz
4	WMTS (Wireless medical telemetry service)	608-614, 1395-1400, 1427-1432 MHz

Table.1.1 Frequency bands allotted by FCC for biomedical implantable devices.

1.2 Literature Review

With just an idea of similarity found in nature, Benoit B. Mandelbrot, also known as the father of fractal geometry, discovered a mathematical equation that can describe the complicated structures around us. All have some self-similarity, from as massive as galaxies to as small as dendrites in neurons. Structures with a well-defined area but an infinite perimeter are known as Fractals. No matter how much you zoom in or out, they will repeat their primary self [1] [2].

The fractal geometry was realized firstly by Nathan Cohen in the making of Fractal Antenna, which proved to be a great discovery in today's world with rapid growth in technology. The need for high-speed communication has to be fulfilled by keeping the compactness of the devices used in mind. Fractal Antenna's primary advantage is its compactness. It has become a massive topic of research. Many recent studies have focused on reducing the size of the fractal antenna and getting broad bandwidth. Manas et al. 2015 mention the various Fractal geometries and their properties that can be utilized to make efficient Fractal antennas. These geometries have non-integer dimensions and have self-similarity. In light of this, researchers have become increasingly interested in implementing this theory to make antennas.

One such research by Sumeet et al. 2016, is based on designing a Fractal antenna with defected ground structure and a random geometry. To further improve its gain and introduce a fractal geometry. This work has been done. Three antennas have been designed

using fractal geometries, namely Sierpinski Gasket, Sierpinski Carpet, and Koch curve [2]. More wideband characteristics and increased gain were found. The proposed antenna can be used in various Military and ultra-wideband communication.[3][5]

Fractal Antennas also have their applications in the biomedical field. Implantable devices are reliable, robust, and cost-effective in diagnosing and even treating many diseases. Research by Tanmaya et al. used Koch curve fractal geometry to design an implantable antenna that showed ultra-wideband characteristics [3].

One such research by Soumyadeep 2018, is based on a slot antenna placed inside a muscle layer. However, the main problem with implantable antennas is that their performance is degraded, and gain becomes less due to the lossy environment provided by the human body[11]. This can be further worked upon for RF energy harvesting and reconfigurable ability. With this, we can make an antenna with compactness, at low cost, and wideband and ultra-wideband characteristics making it useful for satellite communication and various other applications[5][7]. Similarly, research by Suganthi et al. 2012 used Hilbert curve fractal geometry to make the antenna wideband, but the problem of very low gain was there [15]. Research by Chen et al. 2010 for teeth implantable antenna also had very negative gain values [16].

1.3 Chapter Outline

Chapter 1 of this thesis outlines the introduction of my project. It describes the need for a fractal antenna in the modern era of Technology and Engineering. Various frequency bands are allocated to different applications that have been summarized in a tabulated manner. Also, a brief description of our presented work is given along with the Literature Review and has been summarized at the end.

Chapter 2 is dedicated to the Fractals' characteristics leading to the discovery of the Fractal Antenna. Different fractal geometries have been described along with the calculation of their self-similarity dimension. Also, the properties of Fractals that are utilized in making Fractal antennas with the desired qualities have been presented.

Chapter 3 provides details of the proposed antenna based on fractal geometry, namely Sierpinski Gasket Geometry, Sierpinski Carpet Geometry, and Koch Curve Geometry. Details include a brief introduction along with the basic design of the antenna. The design has been simulated on the HFSS 15.0 software, the parametric study has been done, and the results are presented along with the summary at the end.

Chapter 4 provides details of the proposed biomedical implantable antenna based on fractal geometry. Details include a brief introduction along with the basic design of the antenna. The antenna is placed inside different layers models. The design has been simulated on the HFSS 15.0 software, the parametric study has been done, and the results are presented along with the summary at the end.

Chapter 5 provides details of the gain enhancement techniques of the proposed biomedical implantable antenna based on fractal geometry. Details include a brief introduction along with the basic design of the enhancement techniques of the antenna. The design has been simulated on the HFSS 15.0 software, the parametric study has been done, and the results are presented along with the summary at the end.

Chapter 6 of this thesis includes a conclusion, an inference gathered from the compilation of the overall work and observations, and briefly described the scope of future work.

Chapter 7 the last chapter of this thesis, provides the references that have been taken from various sources and research published previously.

1.4 SUMMARY

This chapter provides a brief introduction to the proposed project. It describes the need for the work done in the modern era of technology. Literature Review has been given. Attempts are made to provide an overview of the rest of the thesis in a concised manner.

CHAPTER-2

FRACTAL ANTENNA

2.1 INTRODUCTION

Starting with a brief history, fractal comes from the Latin word “Fractus,” meaning "broken or fractured", which is the property of fractal that no matter how much you break that shape into parts, it will always keep on replicating the original pattern from where we have started. These structures have infinite complexity. In technical terms, these patterns have dimensions that strictly exceed the topological dimensions.

A great mathematician, Benoit Mandelbrot 1975, was the first to define these fractals in his theory of roughness. He wanted to give a mathematical equation for the complicated structures like mountains, coastlines, and the structure of plants, blood vessels, lungs, galaxies, etc. He gave a straightforward equation for representing these highly complex structures or their roughness. The equation is given below:

$$Z_{n+1} = Z_n + C \quad (2.1)$$

In this, we will put a number, square it, add the original number, and repeat the process repeatedly. For some numbers, like 0, it is nothing. For other numbers, it just bounces back and forth like -1, and for the others, it grows to infinity. Furthermore, when this simple equation was implemented using a computer program, a Mandelbrot set was discovered, as given in Figure 2.1. This shape has infinite complexity, which will repeat itself to infinity. No matter how much we zoom in or zoom out.

2.2 FRACTAL THEORY

Fractals have been classified broadly into two types, namely Deterministic and Non-Deterministic Fractals, and further subdivided [2]. A hierarchical chart is given in figure 2.2.

(i) **Deterministic Fractals:** these fractals are made from definite shapes that are scaled or rotated repeatedly to make a structure with very high complexity self-similarity to a considerable extent. They are also known as geometrical fractals. They are further divided into two categories:

(a) **Linear:** They include the repetition of a single shape with alterations in angles or size. Examples of these fractals are Sierpinski Gasket, Sierpinski Carper, Koch curve, Cantor sets, Hilbert curve, etc.

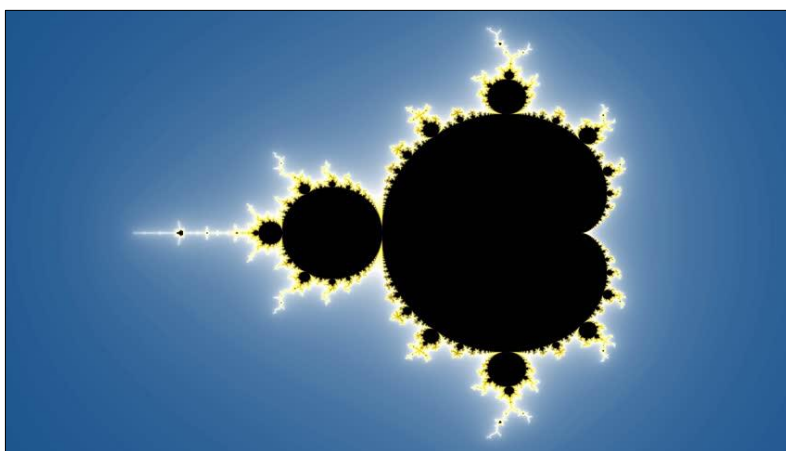


Figure .2.1 Mandelbrot Set [4]

(b) **Non-linear:** they include the repetition of different shapes with alterations in angles or sizes. Examples for the same are Mandelbrot set, Julia set, Strange attractor, etc.

(ii) **Non-Deterministic:** Non- deterministic patterns are very random, but if we zoom on to these random patterns, some similar randomness can be observed. They are also known as Random Fractals. They describe the natural things around us. For example- lightning in the sky, roots of the plants, branches of trees, the circulatory system of humans, the flow of rivers, etc.

Fractal dimensions- One of them introduced by mathematician Felix Hausdorff, thus called Hausdorff Dimensions, is a measure of roughness. There are other dimensions, too, like topological dimensions. It is '0' for sets describing points (0-D), '1' for sets describing lines (1-D), '2' for sets describing surfaces (2-D) having length and width), and '3' for sets

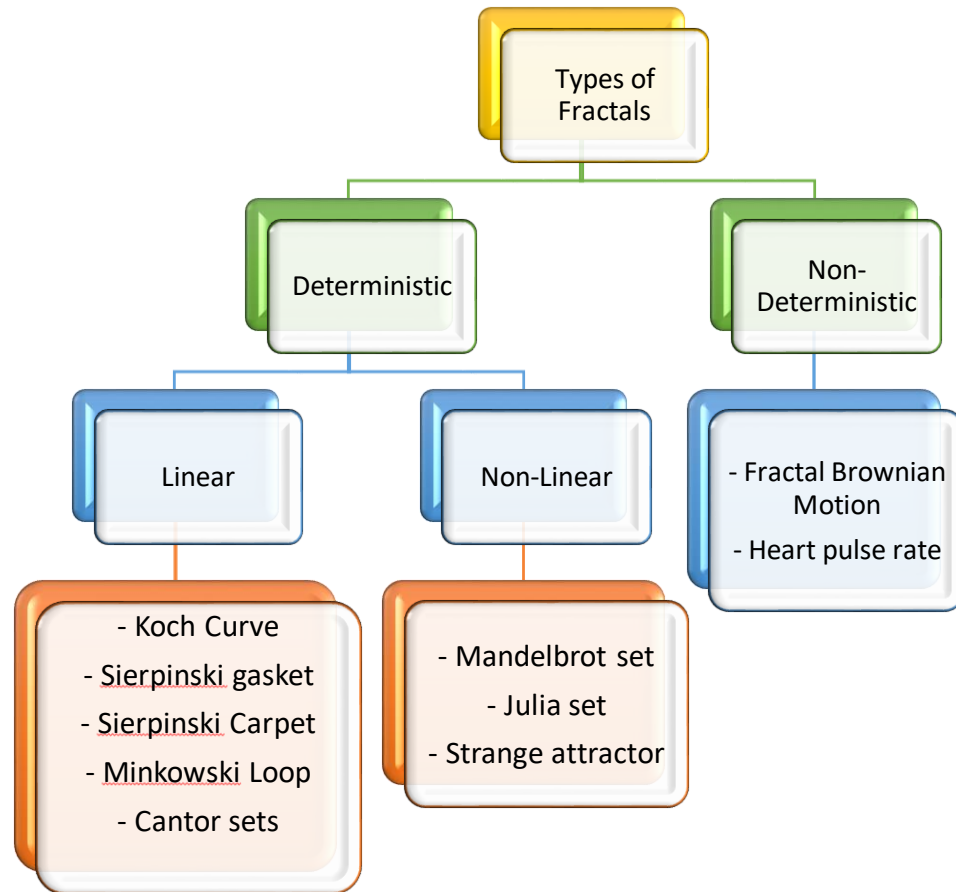


Figure 2.2 Hierarchical chart representing the different types of Fractals.

describing volumes (3-D sets having length, width, and height). However, this changes for fractal sets. The fractal dimension of a set exceeds its topological dimensions. Its values lie between 1 and 2. Their values are non-integer. It is said to be too detailed to be 1-D and too simple to be 2-D.

Fractal Design has commonly two dimensions and components:

A) The Initiator (0th stage) is the basic structure of fractal geometry.

B) The Generator is the structure repeated in a sequential pattern on the initiator in the consequent stages with the different dimensions.

The formula for the self-similarity Dimension is given in equation 2.2.

$$D_s = \frac{\log(N)}{\log\left(\frac{1}{s}\right)} \quad (2.2)$$

Where, 's' is the scaling factor and 'N' is the number of self-similar copies.

2.3 FRACTAL GEOMETRIES

2.3.1 SIERPINKSKI GASKET

This geometry was first discovered by a mathematician, Waclaw Sierpinski. This is the most widely used geometry in antenna designing. It starts with a triangle. Then the midpoints of each side are joined, and a new triangle is formed and removed from the original triangle. [6] The same procedure is done with the new triangles formed repeatedly. This is displayed in Figure 2.3.

From the figure, we can see that the side of the triangle is reduced to half, and thus the scaling factor is $\frac{1}{2}$, and three more copies of the triangle have been generated. According to equation 2.2 The self-similarity dimension is:

$$D_s = \frac{\log(N)}{\log\left(\frac{1}{s}\right)} = \frac{\log 3}{\log 2} = \frac{0.477}{0.301} = 1.585 \quad (2.3)$$

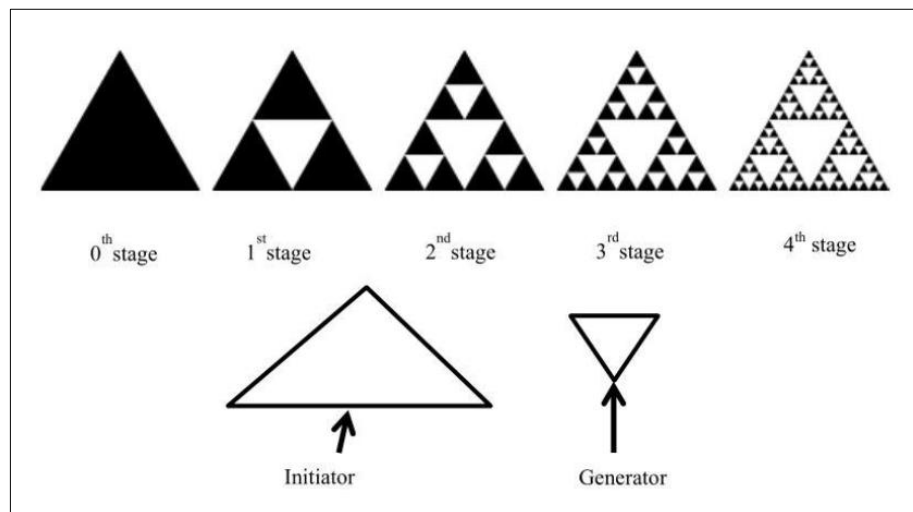


Figure2.3 Sierpinski Gasket

2.3.2 SIERPINSKI CARPET

Similar to the gasket, it is different because it uses squares in place of triangles. A square (initiator) is congruently divided into nine squares in its most straightforward configuration. The central piece is then removed. The same procedure is repeated with the following eight squares.

This is displayed in Figure 2.4.

From the figure, we can see that the side of the square is reduced to one-third, and thus the scaling factor is $1/3$, and 8 more copies of the triangle have been generated. According to equation 2.2 Self-similarity dimension is:

$$D_s = \frac{\log(N)}{\log\left(\frac{1}{s}\right)} = \frac{\log 8}{\log 3} = \frac{0.903}{0.477} = 1.893 \quad (2.4)$$

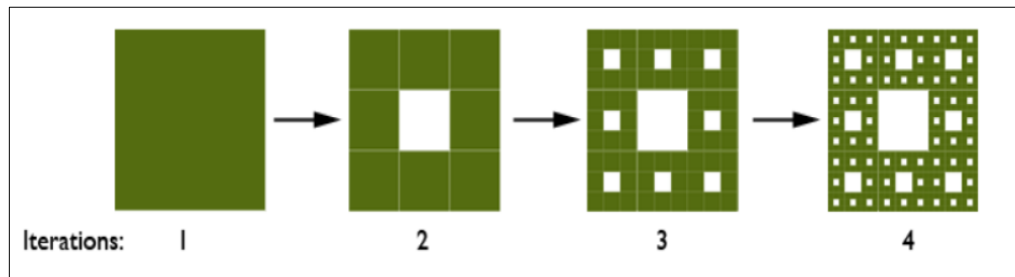


Figure 2.4 Sierpinski Carpet

2.3.3 KOCH CURVE

This geometry is used to reduce the size of a dipole antenna by making a fractal structure which further makes it more wideband in this geometry. A single line is divided into three sections, and the middle one is raised to form a triangle creating four lines now. Again this is repeated with these four lines, and this keeps ongoing. This is displayed in Figure 2.5.

The figure shows that the line is divided into three parts; thus, the scaling factor is $1/3$, and 4 more copies of the line have been generated. According to equation 2.2 Self-similarity dimension is:

$$D_s = \frac{\log(N)}{\log\left(\frac{1}{s}\right)} = \frac{\log 4}{\log 3} = \frac{0.602}{0.477} = 1.262 \quad (2.5)$$

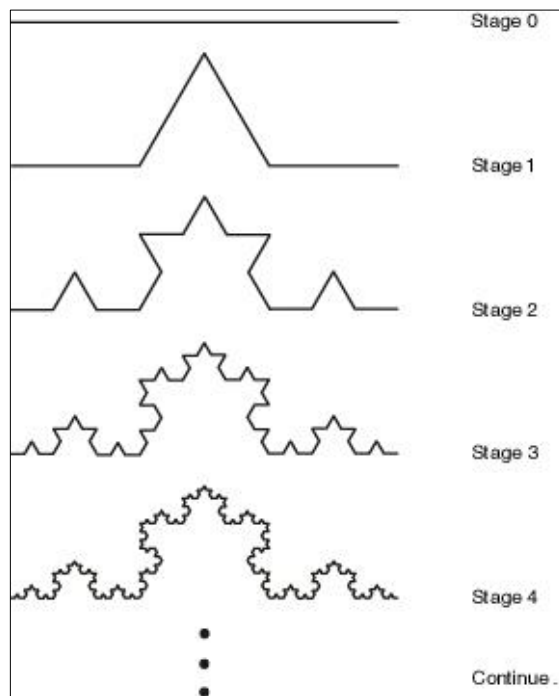


Figure 2.5 Koch Curve

2.4 FRACTAL ANTENNA

A radio astronomer, Nathan Cohen, discovered the fractal antennas in 1995. It all started when his landlord was not allowing him to put a radio antenna on his roof due to its large size. So he decided to make a compact antenna using fractal geometries. However, the made antenna was not only small but with better performance [6].

The central concept behind the fractal antenna was to increase the perimeter or the length of the conductor within a restricted given area or volume that receives or radiates the electromagnetic radiations. To implement this, self-similar structures were used to design an antenna. They are also known as space-filling curves. The different iterations in a design can produce different size geometries that have different electrical lengths and thus resonate at different frequencies, making these antennas wideband or even multi-band [2] [4].

An antenna's wideband and multi-band characteristics make it worthwhile for various applications without putting separate antennas for every application. Fractals have so many different properties that are utilized in making Fractal Antenna. This has been tabulated in Table 2.1.

PROPERTY OF FRACTAL	UTILIZED IN MAKING ANTENNA
Self- Similarity	Wideband and Multiband Antenna
Small dimension	Compact size antenna
Space fillings	Fitting the same electrical length into a compact volume results in antenna miniaturization
No pre-defined characteristics sizes	Frequency independent and multi-wavelength operative antenna
Sharp discontinuities (edges, corners)	Efficient antenna radiation

Table 2.1 Properties of Fractals and their utilization in making Fractal Antenna

❖ Advantages of Fractal Antenna

1. Without altering performance size can be reduced.
2. multiband operations can be done.
3. Improvement in reliability.
4. Naturally broadband, at higher frequencies. non requirement of any matching
5. Components.
6. Reduced costs of installations.
7. Can be operational at multiple wavelengths or frequency independent

❖ Disadvantages of Fractal Antenna

1. Low Gain
2. Too complex geometry
3. After a few iterations, benefits start to diminish soon after.
4. Performance starts to decrease after first little iteration.

➤ Applications of Fractal Antenna

1. **In Building Communication:** Fractal antenna provides universal wideband antenna technology ideal for in-building communication applications. Operating over 150MHz to 6GHz, fractal antennas deliver excellent Omni-directional coverage in a compact form.
2. **Wireless Networks:** Fractal Antenna Systems provide superior advanced antenna technology that enables emerging wireless protocols, such as ZigBee, WiMAX, and MIMO, to deliver their maximum potential.
3. **Universal Tactic Communication:** Future communications systems will use cognitive radios that require vast bandwidths with one antenna.
4. **Mobile Devices:** From PDAs to cellular phones to mobile computing, today's wireless devices require compact, high-performance multi-band antennas. At the same time, packaging constraints demand that each component, especially the antenna, be inherently versatile.
5. **Telematics:** Today, automobiles can have dozens of antennas that provide everything from emergency notification and navigational services to satellite radio and TV. Multiple antennas create performance and form factor challenges and aesthetic design issues.
6. **RFID (Radio-frequency identification):** Fractal antenna system provides a compact, low-cost solution for many RFID applications. Because fractal antennas are small and versatile, they are ideal for more compact RFID equipment [4].

CHAPTER-3

ANTENNA BASED ON
DIFFERENT FRACTAL
GEOMETRIES

3.1 FRACTAL ANTENNA BASED ON SIERPINSKI GASKET GEOMETRY

3.1.1 INTRODUCTION

The proposed antenna is a Wearable Fractal Antenna based on 'Sierpinski Fractal geometry' [6]. This was designed for military applications, and thus, the substrate used in making the antenna is polyester. With Fractal Geometry, the antenna is compact and multiband, operating at the frequency band of (4-10) GHz and (20-33) GHz. Fractional Bandwidth was 90.7 % and 46.6 %, respectively. Hence, the antenna has ultra-wideband characteristics making it useful in Satellite Communication and applications of military, sports, and tracking systems.

Antenna presented previously were wideband but with less gain value [2]. The 0th, 1st, 2nd, and 3rd iteration of the antenna has been shown in Figure 3.1.1. All the designs were implemented using Ansys HFSS 15.0 software, and the simulation results are shown in Figure 3.1.2 and Table 3.1.1

ITERATIONS	TOTAL GAIN (dB)
0th iteration	5.0608
1st iteration	4.9238
2nd iteration	5.0338
3rd iteration	5.2115

Table 3.1.1 Total Gain of various iterations

Using the Return Loss plot given in figure 3.1.2, fractional bandwidth is calculated for each iterations and compared in section 3.4

3.1.2 ANTENNA DESIGN

The antenna proposed in our work is further iterated after the 3rd iteration. Sierpinski

gasket Fractal geometry has been implemented. The triangles formed in the third iteration were further divided into four more triangles, with the size of the sides reduced to half as they were formed by joining the midpoints of the triangle. Also, the triangle at the center is removed from the geometry. The design thus formed is shown in figure 3.1.3, and the dimensions of the antenna are tabulated in table 3.1.2

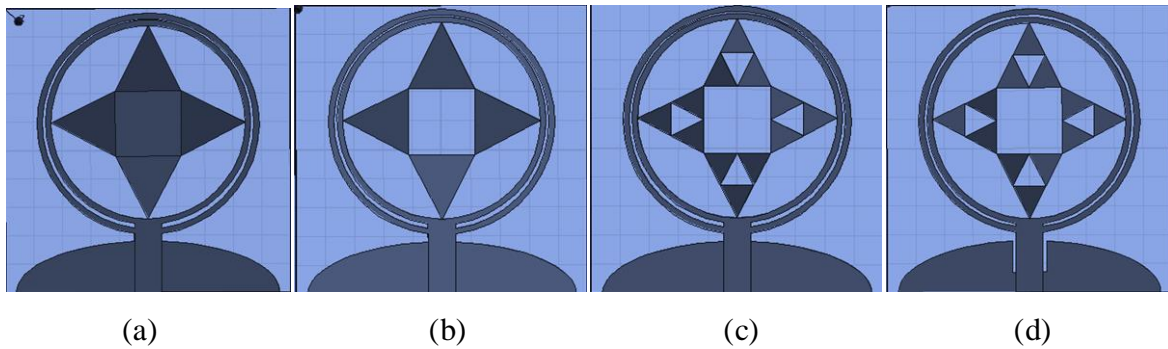


Figure 3.1.1 Antenna design of various iterations (a) 0th iteration (b) 1st iteration (c) 2nd iteration (d) 3rd iteration.

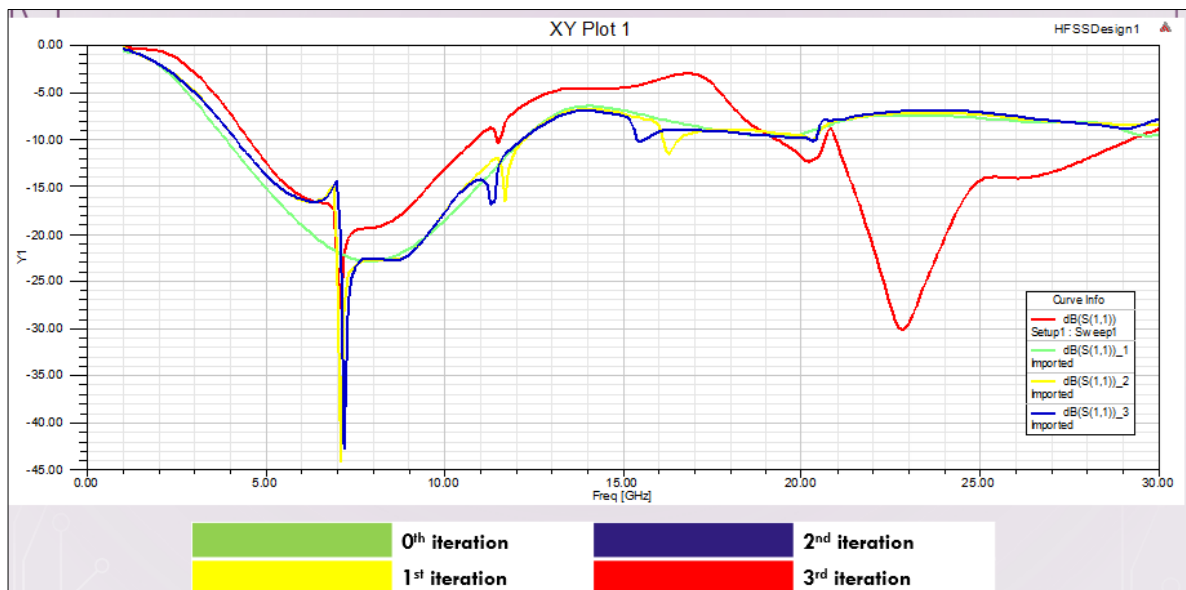


Figure 3.1.2 Return loss plot of the various iterations of the antenna.

The substrate used is Polyester with a dielectric constant of '3.2', and the height of the substrate taken is 1mm. The proposed fractal antenna is of 20 x 20 mm dimension. The

feeding technique used is microstrip line feed of dimension 1.9 x 4.1 mm to get 50ohm characteristic impedance. The ground is in the shape of a semi- ellipse and is known as the defected ground structure of width 20mm and a length of 3.47mm. This is to provide a better impedance matching. A rectangular notch has also been etched out from the ground to improve the impedance bandwidth of dimension 2.2 x 2.4 mm [2]. The design of the proposed antenna is shown in Figure 3.1.3 for both back and front views. Its parametric values are presented in table 3.1.2.

3.1.3 SIMULATION RESULTS

The design is then simulated through the Ansys HFSS 15.0 software over a frequency range of '1 GHz 'to '40 GHz'. The return loss plot and S11 parameter graph are shown in figure 3.4 with the values of the graph, the impedance bandwidth was calculated by the difference between ' higher cut-off frequency' and 'lower cut-off frequency'. Also, the ' center frequency' is calculated by taking an average of both frequency values. To calculate the fractional bandwidth, impedance bandwidth is divided by center frequency [6].

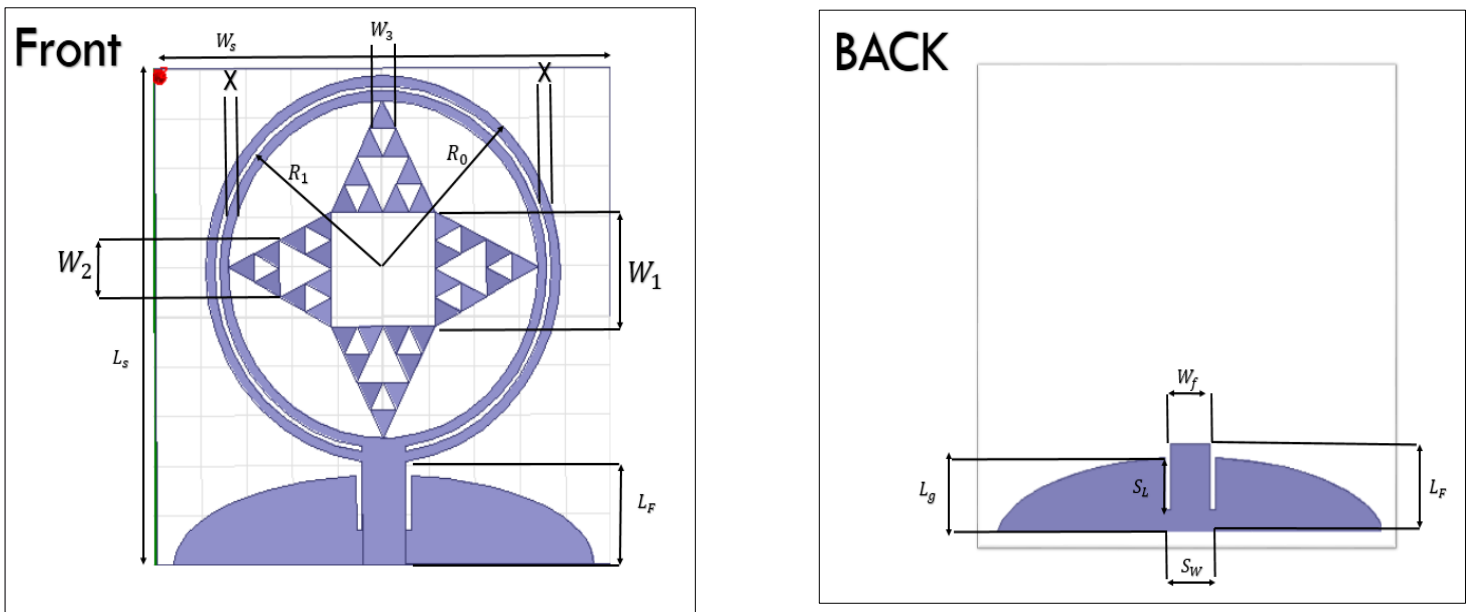


Figure 3.1.3 geometry of proposed Fractal Antenna of both front and back.

PARAMETERS	DESCRIPTION	VALUES
$W_s = W_g$	Width of the substrate	20 mm
L_s	Length of the substrate	20 mm
L_g	Length of the ground plane	3.6 mm
R_0	Radius of the outer ring	7.8 mm
R_1	Radius of the inner ring	7.2 mm
W_F	Width of the feed line	1.9 mm
L_F	Length of the feed line	4.1 mm
W_1	Width of the triangle	4.6 mm
W_2	Width of inner triangle	2.3 mm
W_3	Width of innermost triangle	1.15 mm
X	Space between the circles	0.4 mm
S_w	Width of the slot	2.4 mm
S_L	Length of the slot	2.2 mm

Table 3.1.2 Parametric values of the proposed Fractal Antenna

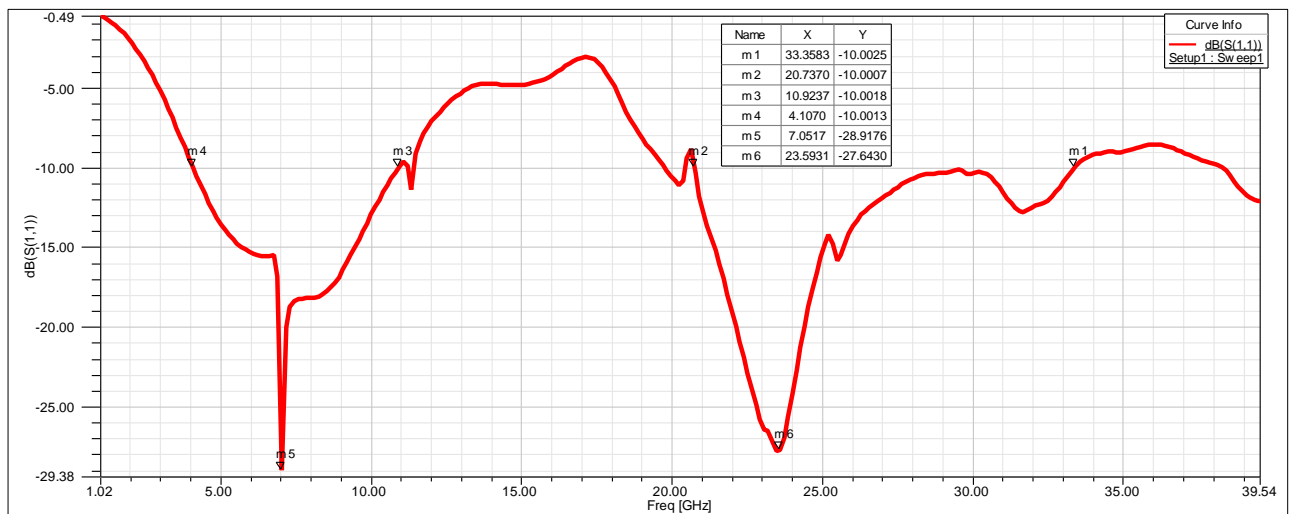


Figure 3.4 return loss plot

As we can see in the graph, two frequency bands are observed that can be operated for various applications. We have calculated the Fractional Bandwidth of both the bands. For band (4-11) GHz, Fractional bandwidth is 90.7 %, and for the (20-33) GHz band, Fractional bandwidth is 46.6%. The VSWR plot and the 3D polar plot is given in figure 3.1.5 and 3.1.6, respectively.

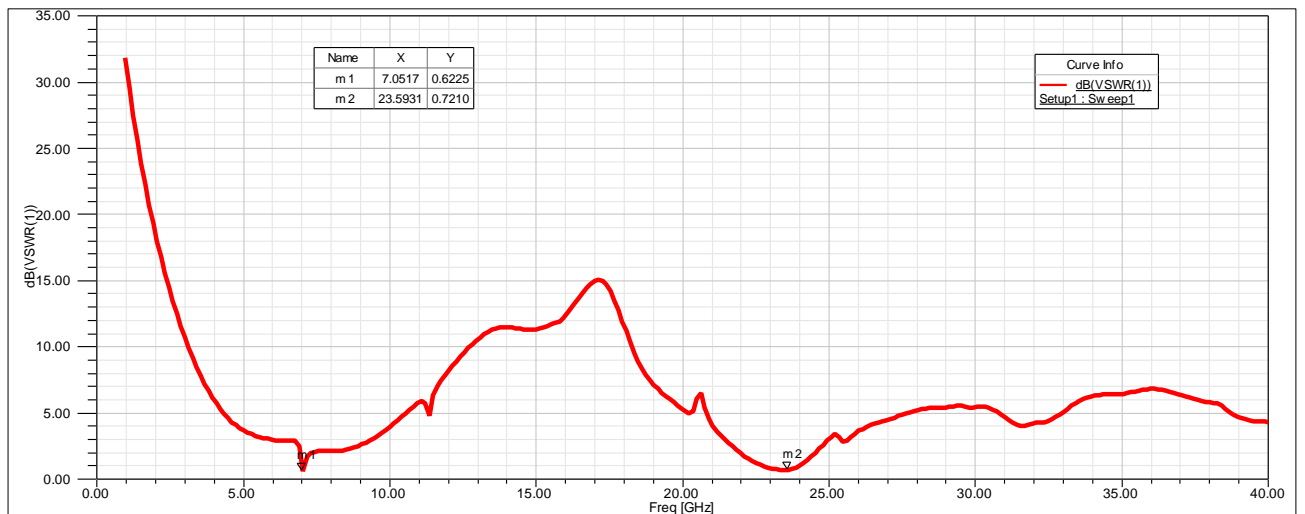


Figure 3.1.5 VSWR plot

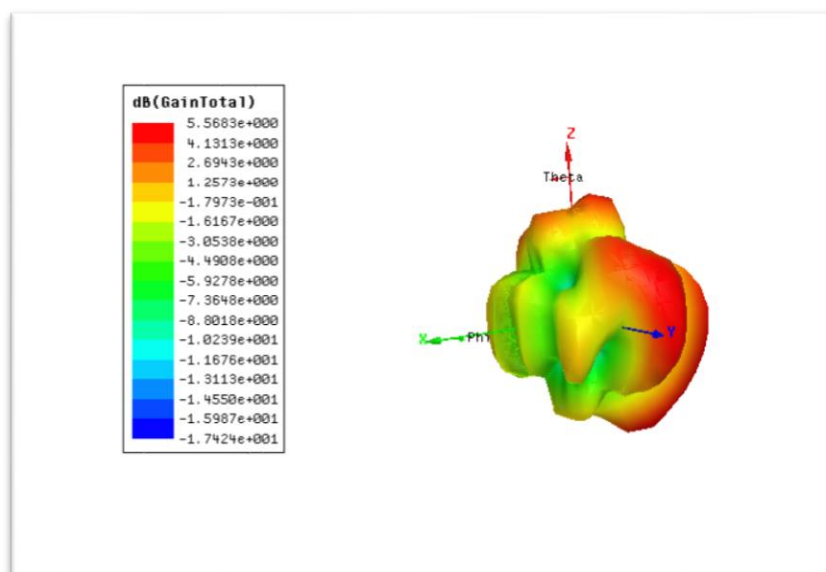


Figure 3.1.6 3-Dimensional polar plot

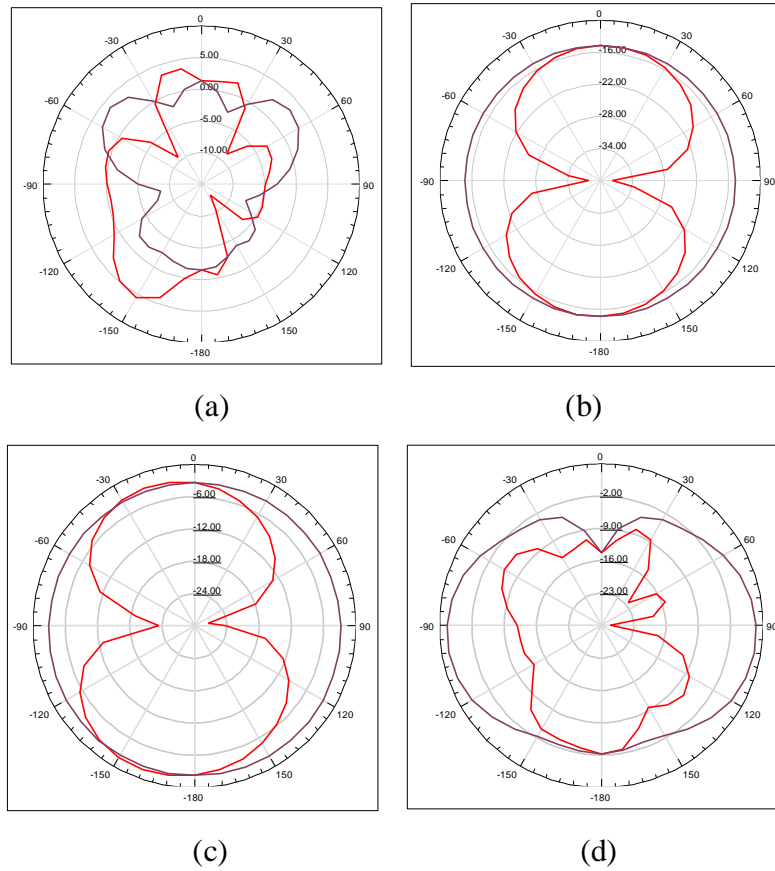
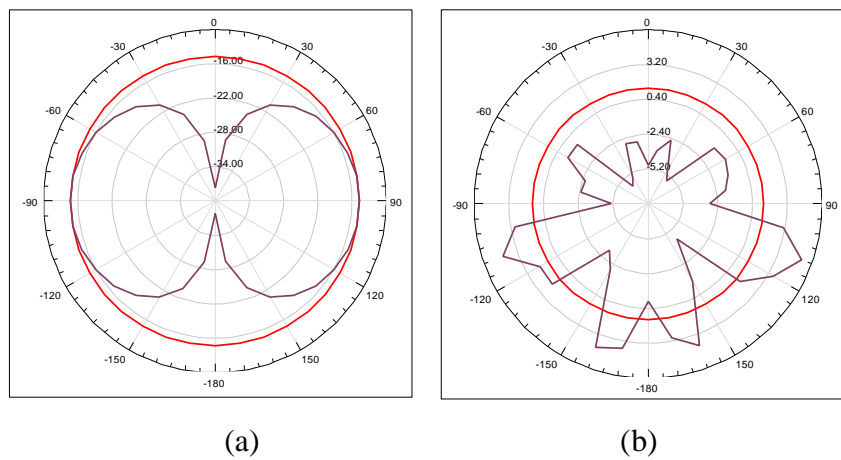


Figure 3.1.7 E field distribution (a) at maximum frequency=30 GHz (b) at minimum frequency=1GHz (c) at first resonating frequency=7.0517GHz (d) at second resonating frequency = 23.5931 GHz



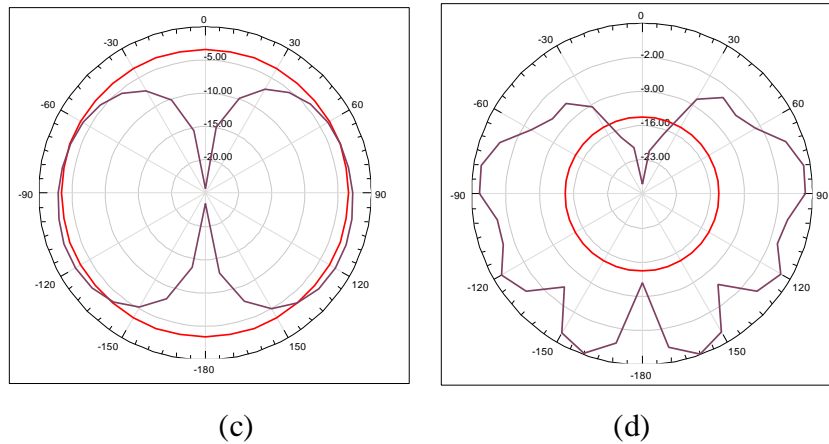


Figure 3.1.8 H field distribution (a) at minimum frequency=1 GHz (b) at maximum frequency=30 GHz (c) at first resonating frequency=7.0517GHz (d) at second resonating frequency = 23.5931 GHz.

The radiation pattern in elevation and the azimuthal plane is shown in Figures 3.1.7 and 3.1.8, respectively. Four different values of frequency have been taken, at maximum, minimum, First resonating frequency and second resonating frequency at $\phi = '0 \text{ degrees}'$ and $'90 \text{ degrees}'$. The red curve represents $'0 \text{ degrees}'$, and the violet curve represents $'90 \text{ degrees}'$.

3.1.4 SUMMARY

A multiband antenna has been designed with wideband and ultra-wideband characteristics. Wideband (4-11) GHz operating at the resonant frequency of 7.05 GHz, which falls in the C and X band of SHF, can be used for Military applications, weather forecasting, and educational purpose (X-band). Ultra-wideband (20-33) GHz operating at the resonant frequency of 23.59 GHz, which falls in the K and Ka-band, can be used for RADAR applications and infrared-astronomy applications [1].

Results have been compared for different iterations on various parameters and are tabulated in Table 3.1.4. Our proposed antenna shows the best result of gain and Fractional bandwidth

ITERATIONS	GAIN (dB)	FRACTIONAL BANDWIDTH	DIP AT S_{11} (dB)	RESONANT FREQUENCY
ITERATION 0	5.0608	103.095 %	-22.8708	8 Ghz
ITERATION 1	4.9238	97.56 %	-44.2287	7.1 Ghz
ITERATION 2	5.0338	97.56 %	-42.8021	7.2 Ghz
ITERATION 3	5.2115	(i) First band = 81.047 % (ii) Second band = 32.898 %	(i) -27.9753 (ii) -30.1421	(i) 7.1 Ghz (ii) 22.8 Ghz
ITERATION 4	5.5683	(i) First band = 90.703 % (ii) Second band = 46.663 %	(i) -28.9176 (ii) -27.643	(i) 7.0517 (ii) 23.5931

Table 3.1.3 comparison of different iterations on the basis of gain and fractional bandwidth

3.2 FRACTAL ANTENNA BASED ON SIERPINSKI CARPET GEOMETRY

3.2.1 INTRODUCTION

The proposed antenna is based on the previous antenna with some alterations. We have used Sierpinski Carpet Fractal geometry and thus designed a wearable Fractal Antenna as we have used polyester as a substrate. With the use of Fractal Geometry, the antenna is compact and also multiband, operating at frequency bands of (5-6.4) GHz, (7-11) GHz, and (19-31) GHz. Fractional Bandwidth was 20 %, 39.15 % and 47.71 % respectively. Hence, the antenna has wideband characteristics making it useful in Satellite Communication and applications of military, sports, and tracking systems [1].

The two designs that are 2nd, 3rd and 4th iteration were implemented by using Ansys HFSS 15.0 software.

3.2.2 ANTENNA DESIGN

The antenna proposed in our work is further iterated after the 1st iteration of the Sierpinski Gasket Fractal geometry antenna presented in 3.1, as shown in figure 3.2.1 (a). The four triangles are replaced by four rectangles of dimension 4.6 mm x 4 mm in the 2nd iteration, as shown in figure 3.2.1 (b). each rectangle formed is congruently divided into nine rectangles. Figure 3.2.1 (c) shows that the central piece is removed, creating 3rd iteration. The same procedure is repeated with the following eight squares, and this is 4th iteration shown in figure (d).

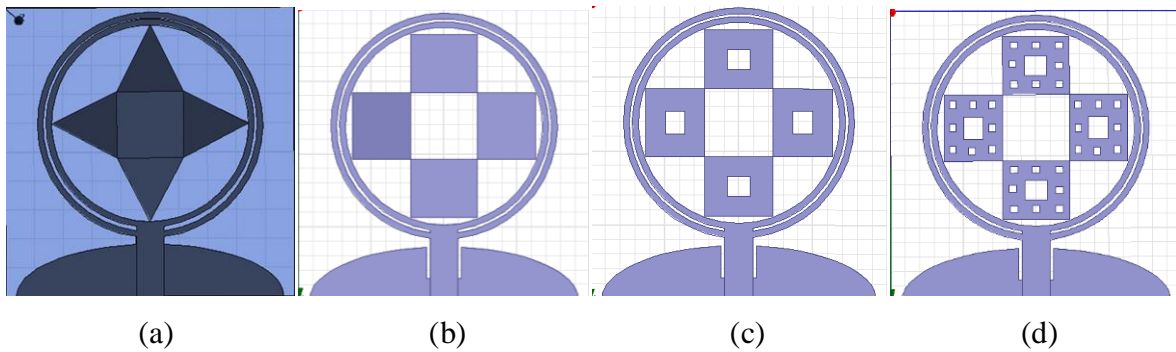


Figure 3.2.1 (a) 1st iteration (b) 2nd iteration (c) 3rd iteration (d) 4th iteration

Rectangles formed in the fourth iteration are of dimension 1.53 x 1.33 mm. The substrate used is Polyester with a dielectric constant of '3.2', and the height of the substrate taken is 1mm. The proposed fractal antenna is of 20 x 20 mm dimension. The feeding technique used is microstrip line feed of dimension 1.9 x 4.1 mm to get 50ohm characteristic impedance. The ground is in the shape of a semi- ellipse and is known as the defected ground structure of width 20mm and a length of 3.47mm. This is to provide a better impedance matching. A rectangular notch of dimension 2.2 x 2.4 mm has also been etched out from the ground to improve the impedance bandwidth.

3.2.3 SIMULATION RESULTS

The design is then simulated through the Ansys HFSS 15.0 software over a frequency range of '1 GHz' to '40 GHz'. The return loss plot, S11 parameter graph is shown in figure 3.2.2 and 3.2.3 for the 1st, 2nd, and 3rd iteration combined and the 4th iteration, respectively.

From the graph values, the impedance bandwidth was calculated by the difference between 'higher cut-off frequency' and 'lower cut-off frequency'. Also, the 'center frequency' is calculated by taking an average of both frequency values. To calculate the fractional bandwidth, impedance bandwidth is divided by center frequency.

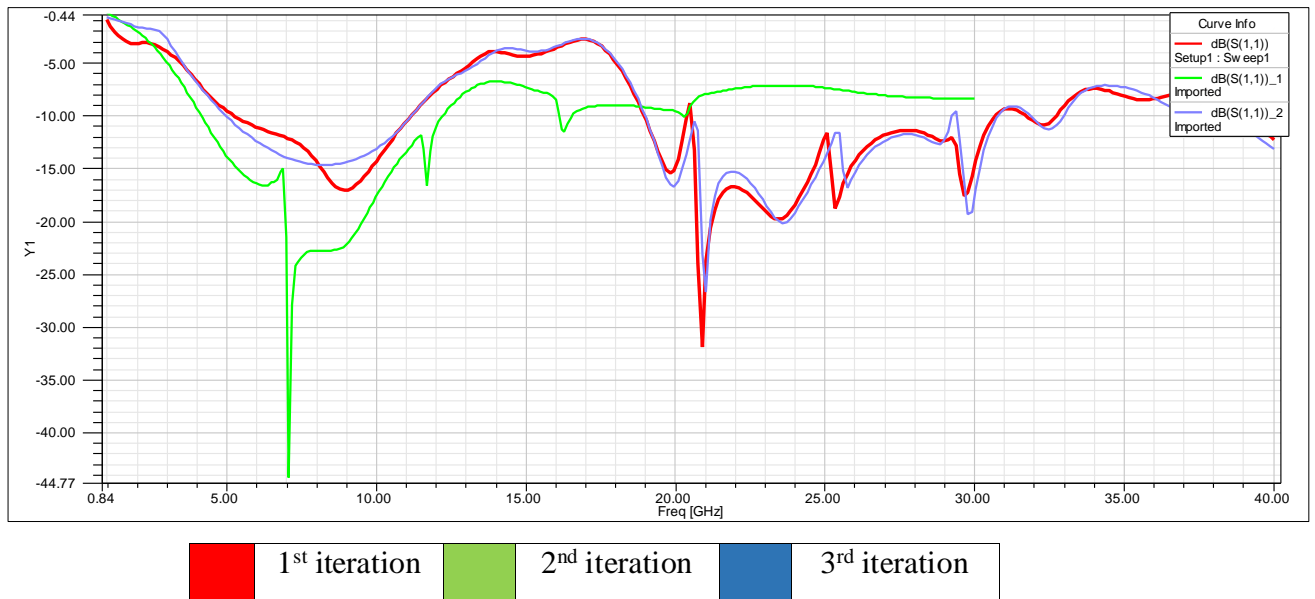


Figure 3.2.2 return loss plot for the first, second and third iterations

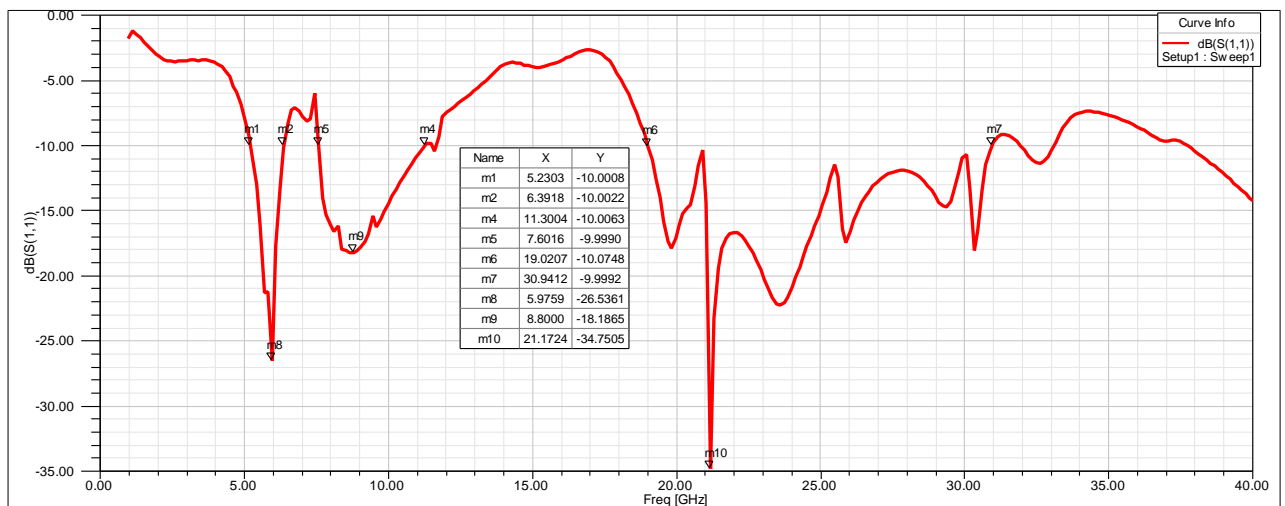


Figure 3.2.3 Return Loss plot for the 4th iteration of the Fractal Antenna

As we can see in the graph, three frequency bands are observed that can be operated for various applications. We have calculated the Fractional Bandwidth of all the bands.

The fractional Bandwidth of band (5.23-6.39) GHz is 20%. The fractional Bandwidth of band (7.6-11.3) GHz is 39.15 %. The fractional Bandwidth of band (19.02 – 30.94) GHz is 47.71 %.

The VSWR plot and the 3D polar plot is given in figure 3.2.4 and 3.2.5, respectively.

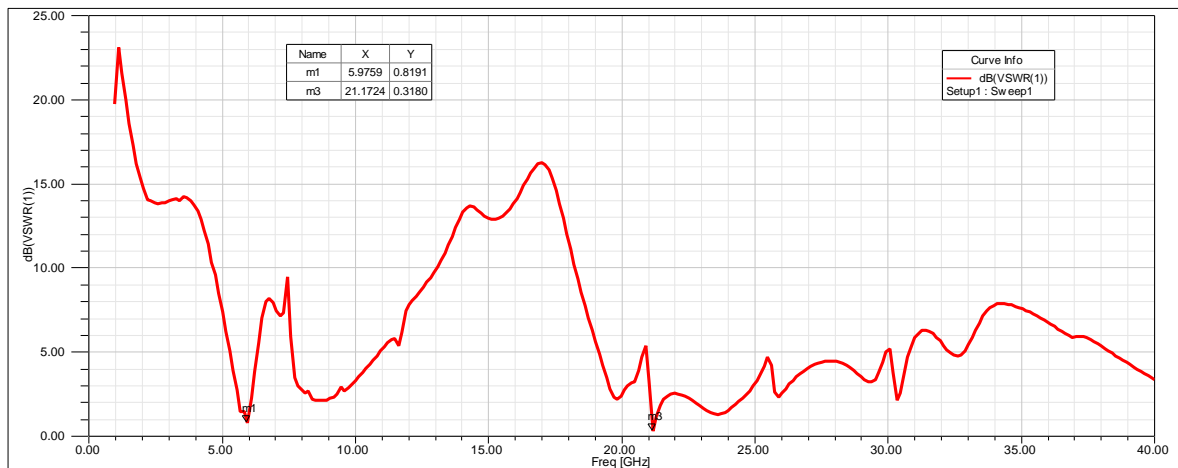


Figure 3.2.4 VSWR plot

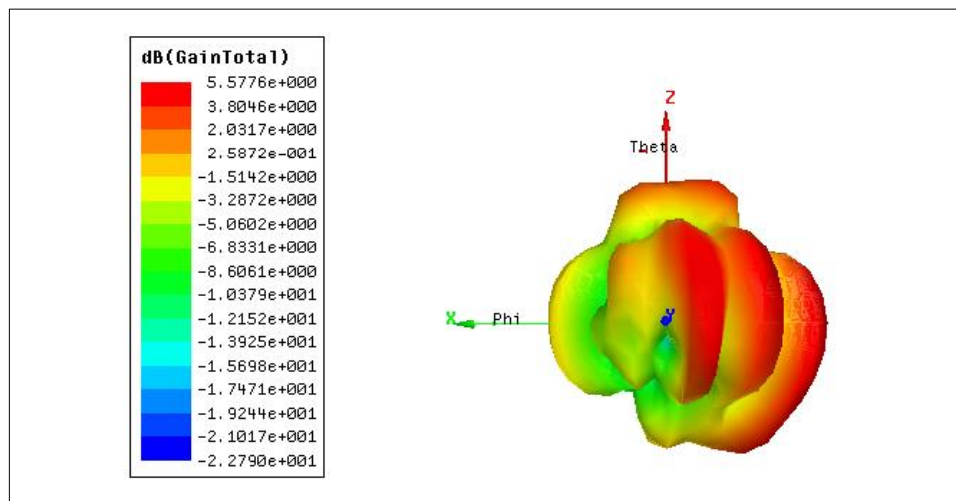
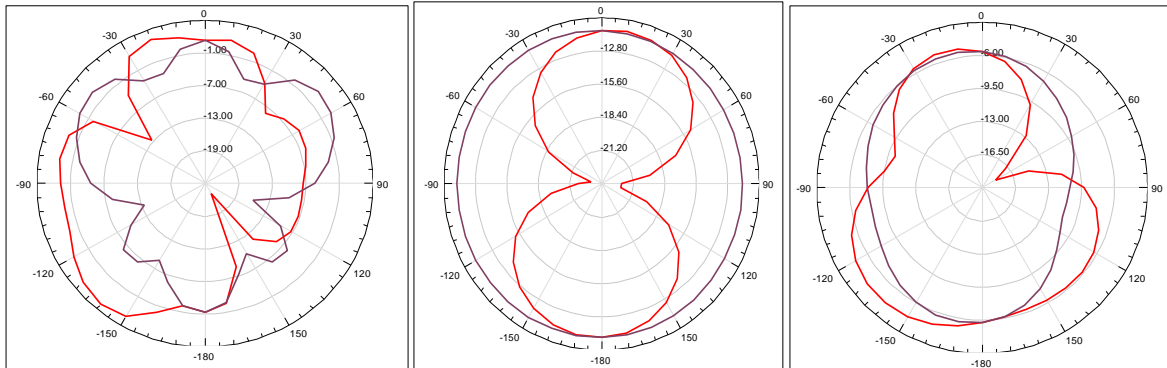


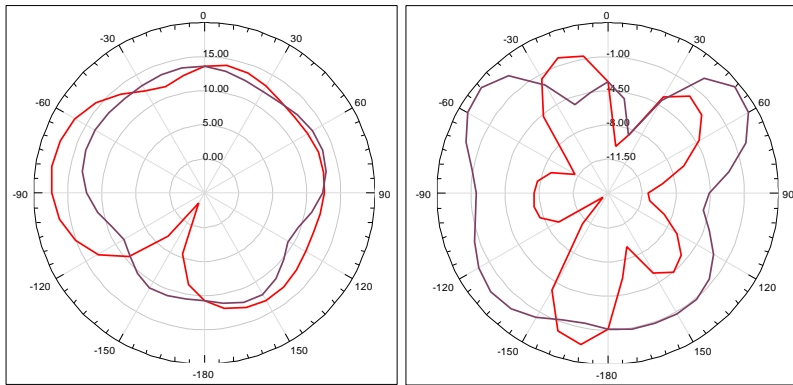
Figure 3.2.5 3-dimensional Polar Plot



(a)

(b)

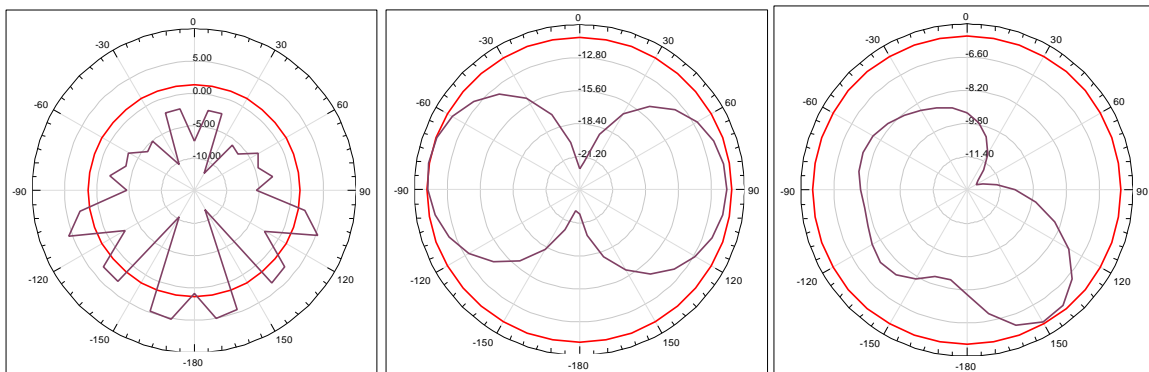
(c)



(d)

(e)

Figure 3.2.6 E field distribution (a) at maximum frequency=30 GHz (b) at minimum frequency=1GHz (c) at first resonating frequency=5.97GHz (d) at second resonating frequency = 8.8 GHz (e) at third resonating frequency = 21.1724



(a)

(b)

(c)

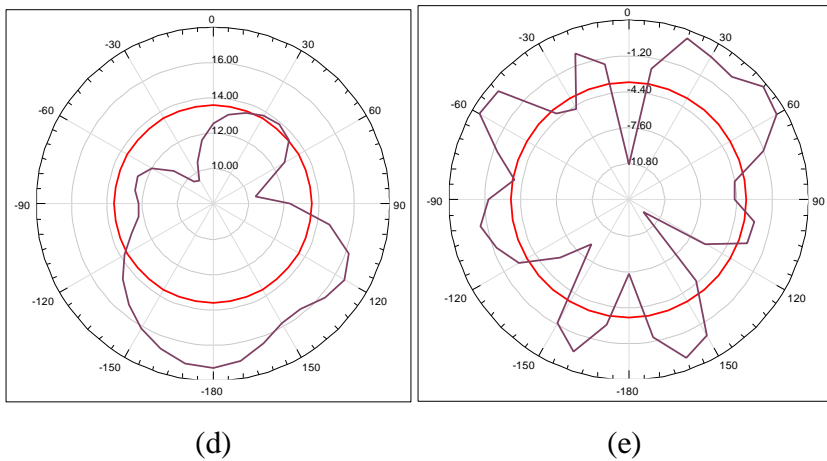


Figure 3.2.7 H field distribution (a) at maximum frequency=30 GHz (b) at minimum frequency=1GHz (c) at first resonating frequency=5.97GHz (d) at second resonating frequency = 8.8 GHz (e) at third resonating frequency = 21.1724

The radiation pattern in elevation and the azimuthal plane is shown in Figures 3.2.6 and 3.2.7, respectively. Four different values of frequency have been taken, at maximum, minimum, First resonating frequency, second resonating, and third resonating frequency at $\phi = '0 \text{ degrees}'$ and $'90 \text{ degrees}'$. The red curve represents $'0 \text{ degrees}'$, and the violet curve represents $'90 \text{ degrees}'$.

3.2.4 SUMMARY

A multiband antenna has been designed with wideband characteristics. Wideband (5.23-6.39) GHz operating at the resonant frequency of 5.97 GHz, which falls in the C band of SHF, can be used for Military applications. The next wideband, (7.6-11.3) GHz operating at the resonant frequency of 8.8 GHz, which falls in the X band of SHF, can be used for Military applications, weather forecasting, and educational purpose. Next next wideband (19.02-30.94) GHz operating at the resonant frequency of 21.1724 GHz, which falls in the K and Ka-band, can be used for RADAR applications and infrared-astronomy applications. Results have been compared for different iterations on various parameters and are tabulated in Table 3.2.1. Our proposed antenna shows the best result of gain and tri-band characteristics

ITERATIONS	GAIN (dB)	FRACTIONAL BANDWIDTH	DIP AT S_{11} (dB)	RESONANT FREQUENCY
ITERATION1	4.9238	97.56 %	-44.2287	7.1 GHz
ITERATION 2	5.0857	(i) First band = 76.113 % (ii) Second band = 21.18 %	(i) -14.6669 (ii) -26.6155	(i) 8.13 GHz (ii) 21.04 GHz
ITERATION 3	4.7551	(i) First band = 71.62 % (ii) Second band = 39.28 %	(i) -17.0612 (ii) -31.8388	(i) 8.93 GHz (ii) 20.9 GHz
ITERATION 4	5.5776	(i) First band = 19.96 % (ii) Second band = 39.15 % (iii) Third band = 47.71 %	(i) -26.5361 (ii) -18.1865 (iii) -34.7505	(i) 5.98 GHz (ii) 8.8 GHz (iii) 21.17 GHz

Table 3.2.1 comparison of different iterations on the basis of gain and fractional bandwidth

3.3 FRACTAL ANTENNA BASED ON KOCH CURVE GEOMETRY

3.3.1 INTRODUCTION

The proposed antenna is based on the previous antenna with some alterations. We have used Koch Curve Fractal geometry and thus designed a wearable Fractal Antenna as we have used polyester as a substrate. With Fractal Geometry, the antenna is compact and multiband, operating at the frequency band of (4-11) GHz and (20-28) GHz. Fractional Bandwidth was 82.11 % and 29.79 %, respectively. Hence, the antenna has wideband and ultra-wideband characteristics making it useful in Satellite Communication and applications of military, sports, and tracking systems.

The two designs that are 2nd iteration and the 3rd iteration were implemented using Ansys HFSS 15.0 software.

3.3.2 ANTENNA DESIGN

The antenna proposed in our work is further iterated after the 1st iteration of the Sierpinski Gasket Fractal geometry antenna presented in Chapter 3, as shown in figure 3.3.1 (a). A star geometry replaces the four triangles by rotating the copy of each star to 180 degrees and placing it over another forming a star in the 2nd iteration, as shown in figure 3.3.1 (b). three outer sides of the star are again iterated to create three more starts. This is done to all the previous four stars. Also, a star is removed from the center of each one, as shown in figure 3.3.1 (c), forming 3rd iteration.

The substrate used is Polyester with a dielectric constant of 3.2, and the height of the substrate taken is 1 mm. The proposed fractal antenna is of 20 x 20 mm dimension. The feeding technique used is micro- stripline feed of measurement 1.9 x 4.1 mm to get 50ohm characteristic impedance. The ground is in the shape of a semi- ellipse and is known as a defected ground structure of width 20mm and a length of 3.47mm. This is to provide a better impedance matching. A rectangular notch of dimension 2.2 x 2.4 mm has also been etched out from the ground to improve the impedance bandwidth.

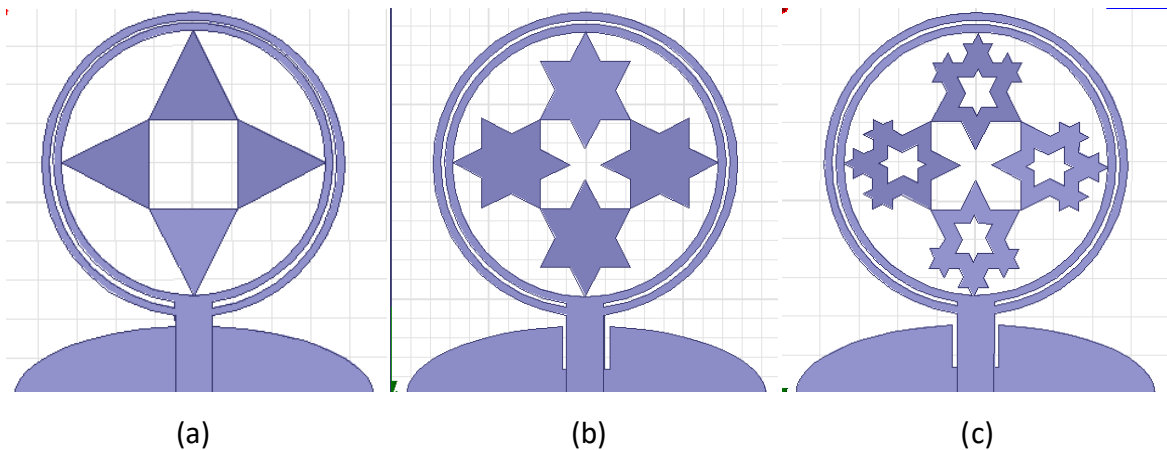


Figure 3.3.1 (a) 1st iteration (b) 2nd iteration (c) 3rd iteration

3.3.3 SIMULATION RESULTS

The design is then simulated through the Ansys HFSS 15.0 software over a frequency range of '1 GHz to 40 GHz'. The return loss plot, S11 parameter graph is shown in figures 3.3.2 and 5.3 for the 1st and 2nd iterations combined and for the 3rd iteration

respectively. From the graph values, the impedance bandwidth was calculated by the difference between 'higher cut-off frequency' and 'lower cut-off frequency.' Also, the 'center frequency' is calculated by taking an average of both frequency values. To calculate the fractional bandwidth, impedance bandwidth is divided by the center frequency

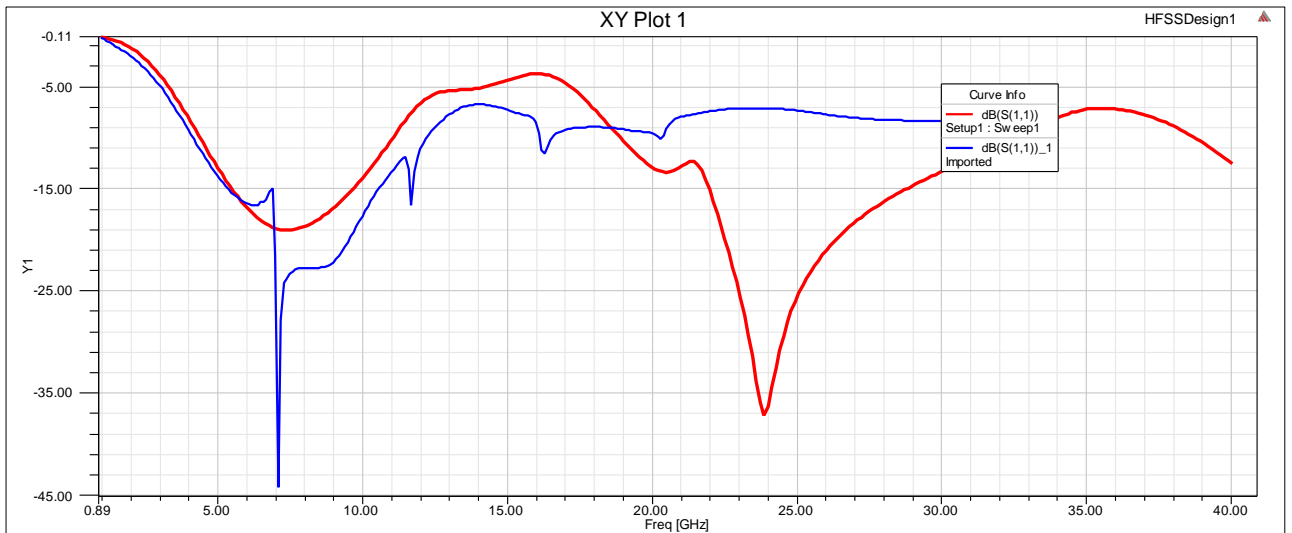


Figure 3.3.2 return loss plot for the first (blue) and second (red) iterations

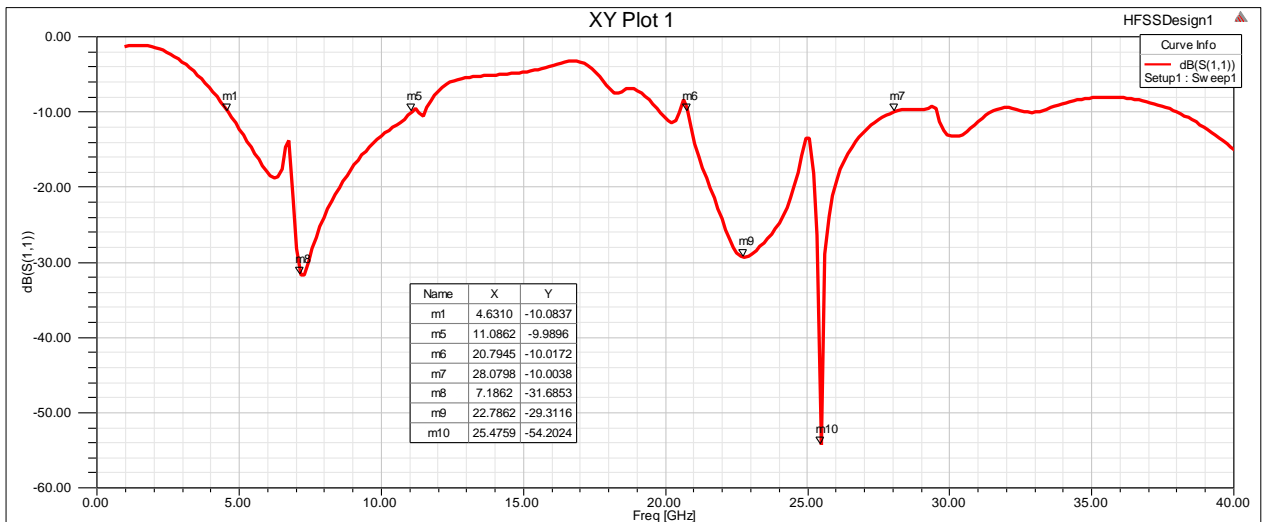


Figure 3.3.3 Return Loss plot for the 3rd iteration of the Fractal Antenna

As we can see in the graph, three frequency bands are observed that can be operated for various applications. We have calculated the Fractional Bandwidth of all the bands.

Fractional Bandwidth of band (4.63-11.08) GHz of 82.11 %. Fractional Bandwidth of band

(20.79 – 28.07) GHz of 29.79%. The VSWR plot and the 3D polar plot is given in figure 3.3.4 and 3.3.5, respectively. The radiation pattern in elevation and the azimuthal plane is shown in Figures 3.3.6 and 3.3.7, respectively. Four different frequency values have been taken at maximum, minimum, First resonating frequency, and second resonating frequency at phi = '0 degrees' and '90 degrees.' The red curve represents '0 degrees', and the violet curve represents '90 degrees.'

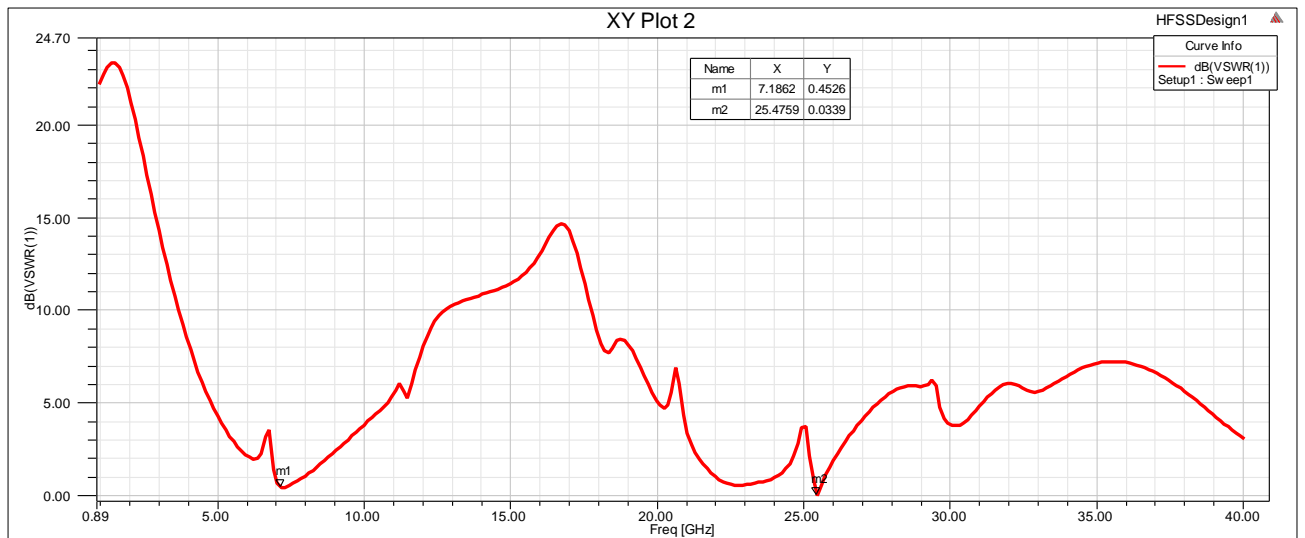


Figure 3.3.4 VSWR plot

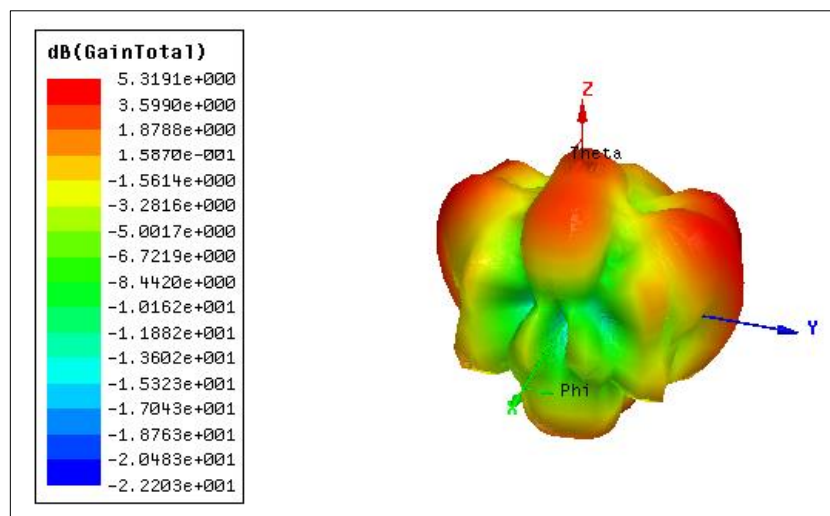


Figure 3.3.5 3-Dimensional polar plot

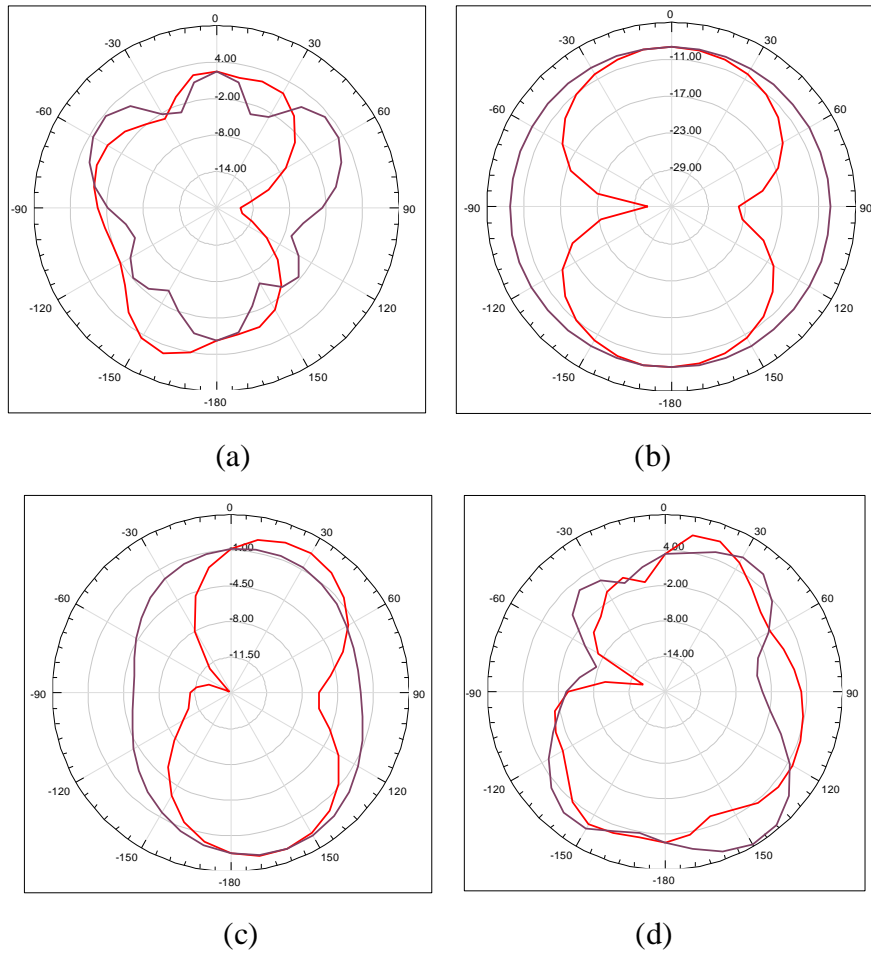
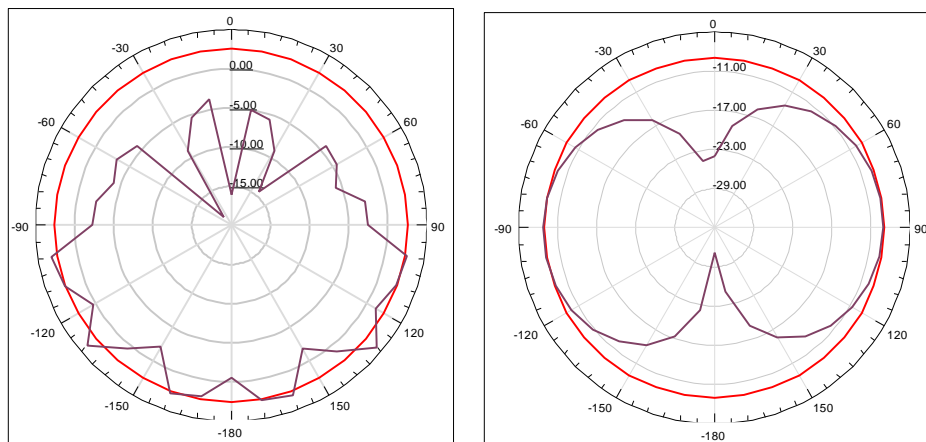


Figure 3.3.6 E field distribution (a) at maximum frequency=30 GHz (b) at minimum frequency=1GHz (c) at first resonating frequency= 7.19GHz (d) at second resonating frequency = 25.48 GHz



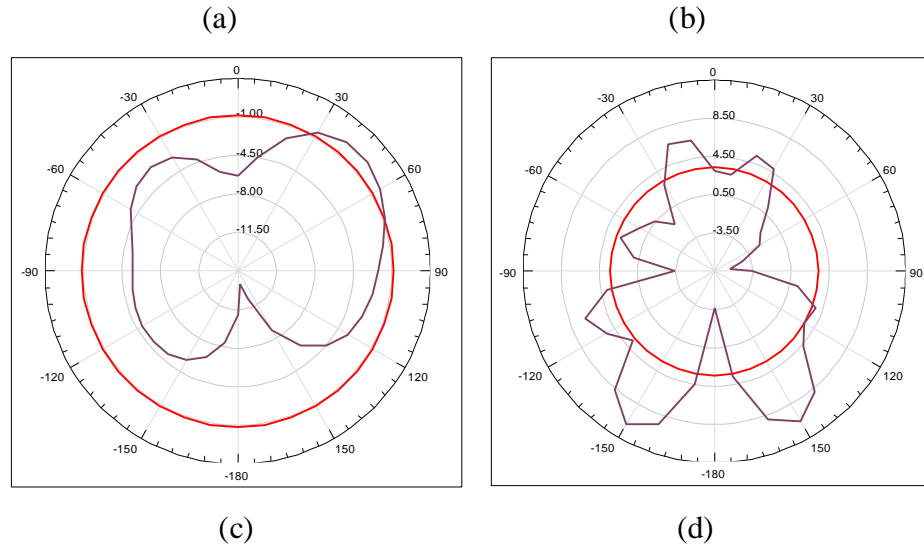


Figure 3.3.7 H field distribution (a) at maximum frequency=30 GHz (b) at minimum frequency=1GHz (c) at first resonating frequency= 7.19GHz (d) at second resonating frequency = 25.48 GHz

3.3.4 SUMMARY

A multiband antenna has been designed with wideband and ultra-wideband characteristics. Ultra-wideband (4.63 – 11.08) GHz operating at a resonant frequency of 7.1862 GHz, which falls in the C and X band of SHF, can be used for Military applications, weather forecasting, and educational purpose (X-band). Wideband (20.79-28.07) GHz operating at a resonant frequency of 25.4759 GHz, which falls in the K band , can be used for RADAR applications and infrared-astronomy applications.

Results have been compared for different iterations on various parameters and are tabulated in Table 3.3.1. Our proposed antenna shows the best result of gain and dual-band characteristics.

ITERATIONS	GAIN (dB)	FRACTIONAL BANDWIDTH	DIP AT S_{11} (dB)	RESONANT FREQUENCY
ITERATION1	4.9238	97.56 %	-44.2287	7.1 GHz
ITERATION 2	4.7722	(i) First band = 87.05 % (ii) Second band = 53.28 %	(i) -19.0449 (ii) -37.0991	(i) 7.455 GHz (ii) 23.86 GHz
ITERATION 3	5.3191	(i) First band = 82.113 % (ii) Second band = 29.79 %	(i) -31.6853 (ii) -54.2024	(i) 7.19 GHz (ii) 25.48 GHz

Table 3.3.1 Comparison of different iterations on the basis of gain and fractional bandwidth

CHAPTER-4

BIOMEDICAL

IMPLANTABLE ANTENNA

USING FRACTAL

GEOMETRY

4.1 INTRODUCTION

Implanted medical devices have improved healthcare quality by continuously monitoring the patients. Glucose monitoring, blood pressure monitoring, anticoagulation testing, electrocardiography, heart rate, oxygen monitoring, etc., are some of the applications of these devices [10] [13]. There are alert alarms linked with these continuous monitoring systems that can effectively care for the patients. With this facility, patients' hospitalization time is reduced and can be treated at home, making the procedure cost-effective. Some examples are maternity care, pediatric care, old-aged bedridden care, etc. An effective home healthcare monitoring system will give accurate information about the patients' internal body to an external device. Figure 4.1 shows the features of one such system.

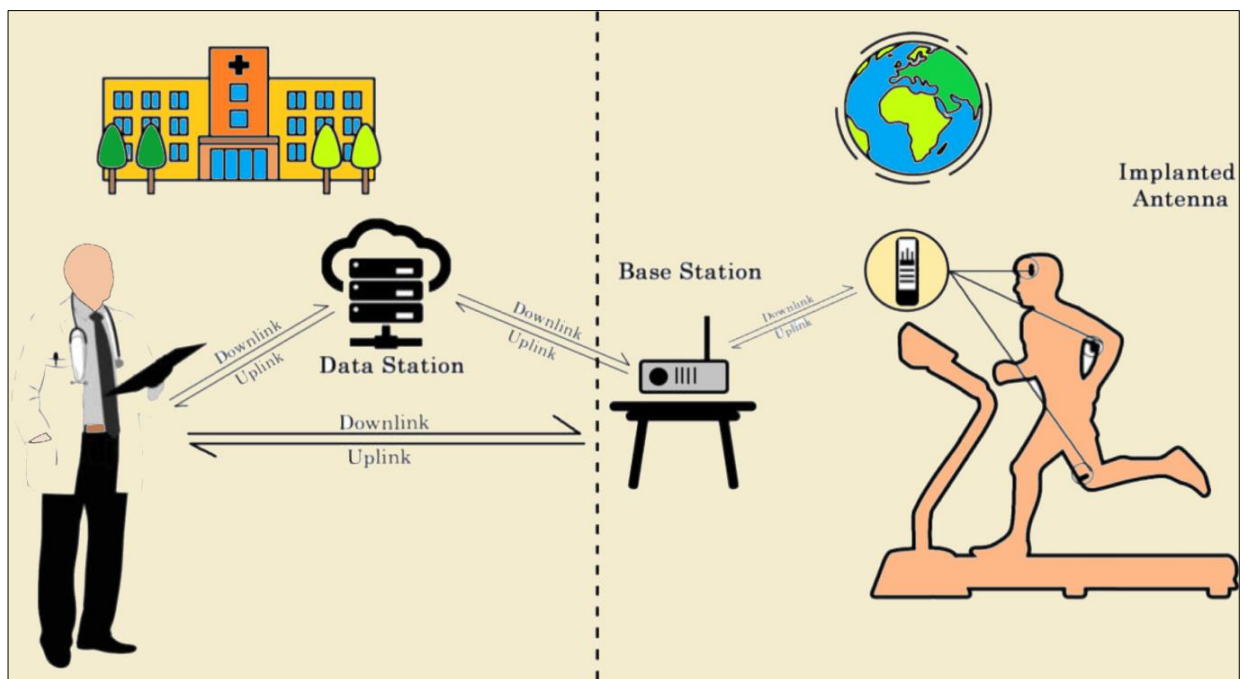


Figure.4.1 Wireless Communication of Implantable Antenna System [13]

(i) Base Station - is the external device that communicates with the implanted device from a receiver module connected with an internet modem. It also consists of a control device to drive the system and store the data.

(ii) Channel - The system's performance depends on the propagation path of electromagnetic waves from implanted to receiving antenna. Multi-path propagation and

scattering EM waves by striking the nearby objects in the room are important aspects to focus on for a reliable healthcare system.

(iii) Human body - As the implantable device is placed inside the human body, it creates a lossy and dispersive environment for an implanted antenna, affecting the system's performance and thus making the designing of the antenna somewhat complex.

(iv) Implanted Device - consists of an antenna, battery, sensors and actuators, insulation, etc., as shown in Figure 4.2. and described below.

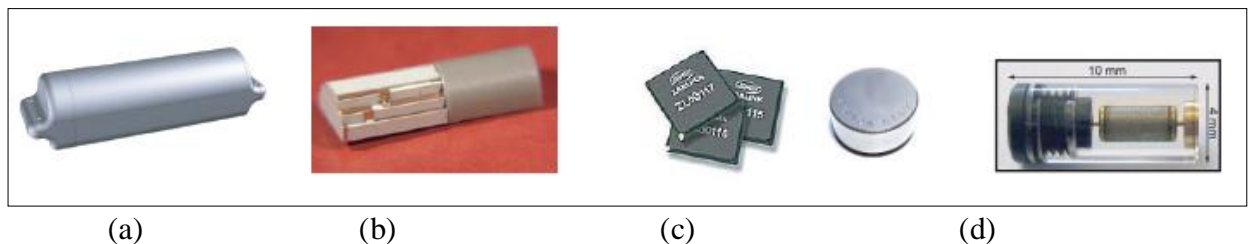


Figure.4.2 Parts of IMD: (a) Insulation (b) implantable antenna (c) power supply and electronics circuits (d) Bio-sensors and Bio-actuators.

(a) Insulation - This layer around the antenna is biocompatible to prevent any reaction within the body. As the human body is a hostile environment for radio waves, thus this type of insulation is essential for proper wireless communication [13].

(b) Implantable antenna - This antenna is responsible for transmitting and receiving the signals and is placed inside the human body. For minimum invasiveness, the antenna should be made small and lightweight. Different techniques like meandered slots, fractals, etc., are used to achieve this. The antenna should also be flexible to prevent the breakage of the antenna with any movement of the body part of the muscle.

(c) Power supply and electronics circuits - The device's power supply determines its lifetime and occupies the most significant part of the device. It can have various sources like energy harvesting, internal batteries, or wireless power transfer. The electronic

circuitry is responsible for the functioning and signal processing of the system. It transfer and stores the information.

(d) Bio-sensors and Bio-actuators - are the monitoring devices that determine the application of the IMD. They measure different quantities like glucose, temperature, pH, etc. Power limitations - Heat is generated from the device, which can be hazardous for the human body. FCC has set the limitation of SAR (specific absorption rate) value to be 1.6 W/kg averaged over 1 gram of human tissue [13].

4.2 ANTENNA DESIGN

The biocompatible implantable antenna configuration comprises two rectangular slots of equal width w , shown in Fig.4.3(a). These slots with the outer dimensions as $L1$ and inner dimensions as $L2$ are fabricated on a $10\text{ mm} \times 10\text{ mm}$ polyethylene substrate with dielectric constant (ϵ_r) 2.25 and loss tangent 0.001. A superstrate layer of alumina having a high dielectric constant of 9.4 and loss tangent 0.006 is placed over the antenna. High values of the dielectric constant of the superstrate material stabilize fluctuations around the antenna due to effective permittivity. It also decouples the antenna from the lossy surrounding [11].

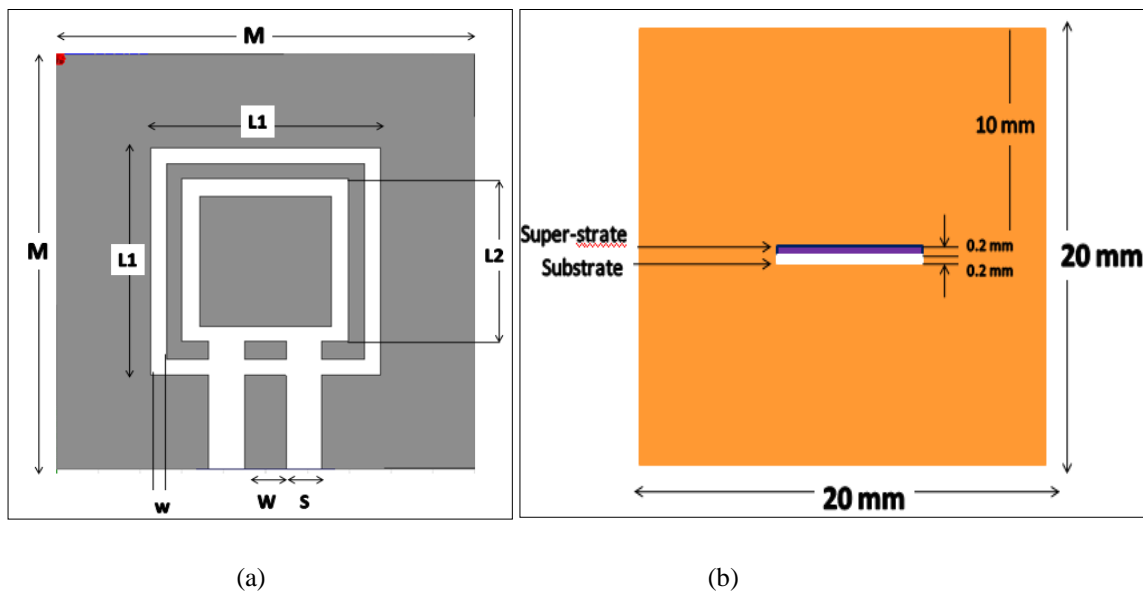


Figure. 4.3 (a) Geometry of antenna (0th iteration) (b) Antenna placed inside muscle layer.

Substrate and superstrate materials are chosen based on impedance matching, minimum reflection, and biocompatibility. Keeping in mind the flexibility, both superstrate and substrate thickness is maintained at 0.2 mm. The Total dimension of the proposed antenna is 10 mm \times 10 mm. Here, the Co-Planar Waveguide (CPW) feed is used for 50 Ω impedance matching by using appropriate trace width (W) and ground plane spacing (S). Fig. 4.2(b) shows the placement of the proposed antenna inside a single-layer human-muscle model. Table 4.1 shows all the design parameters of the implantable slot antenna.

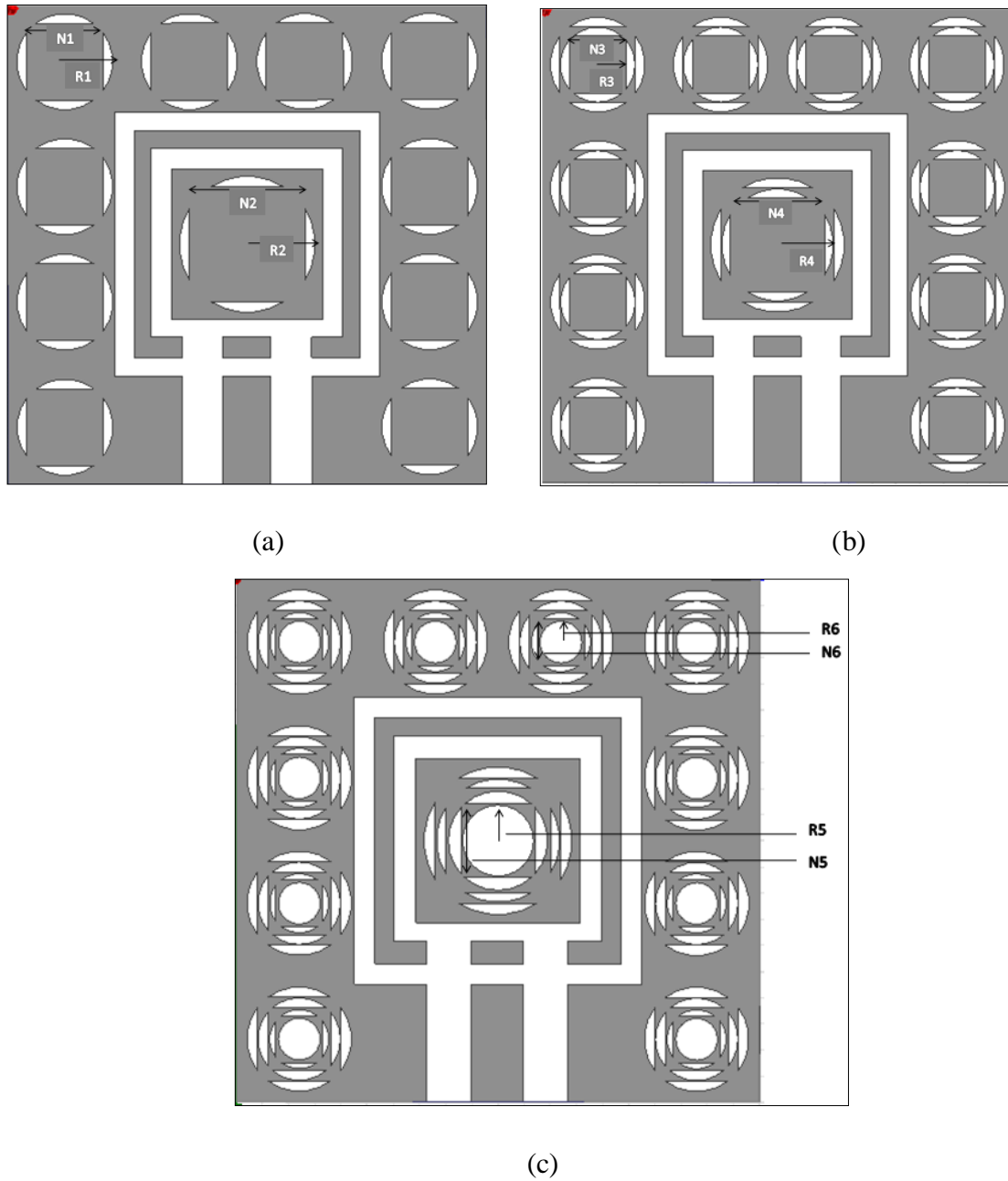
S. No.	Parameters	Description	Values
1.	M	Width and length of substrate	10 mm
2.	L1	Outer rectangular slot	5.5 mm
3.	L2	Inner rectangular slot	4 mm
4.	W	Trace width	0.5 mm
5.	S	Ground plane spacing	1 mm
6.	w	Width of the slot	0.85 mm

Table 4.1 Design parameters of the implantable antenna.

Considering the antenna in figure 4.3 (a) as the 0th iteration, we will further design the fractal antenna using Inscribed square circular fractal geometry. In the first iteration, as shown in Figure 4.4 (a), ten circles of radius 1 mm are removed from three sides, creating slots. One more circle of radius 1.4 mm is drawn from the center. The next step is to make squares of 1.6 mm dimension at the center of each circle and 2.4 mm at the center circle. This completes our first iteration. Similarly, further iterations are done as shown in figure 4.4 (b) and (c), and the dimensions for the same are given in Table 4.2.

S. No.	Parameters	Values (mm)
1.	R1	1
2.	N1	1.6
3.	R2	1.4
4.	N2	2.4
5.	R3	0.8
6.	N3	1.2
7.	R4	1.2
8.	N4	2
9.	R5	0.6
10.	N5	0.9
11.	R6	1

Table 4.2 Design parameters of the proposed fractal antenna.

Figure 4.4 (a) 1st iteration (b) 2nd iteration (c) 3rd iteration

4.3 SIMULATION RESULTS

The design is then simulated through the Ansys HFSS 15.0 software over a frequency range of '1 GHz' to '5 GHz'. The return loss plot and S11 parameter graph are shown in Figures 4.5 and 4.6 for the 1st and 2nd iteration combined and for the 3rd iteration, respectively.

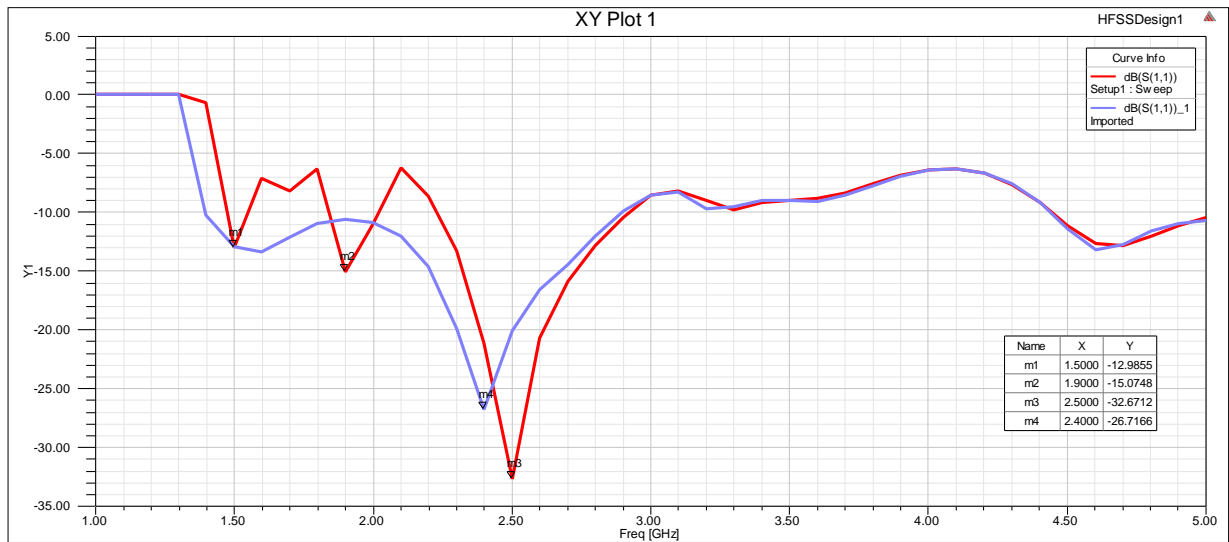


Figure 4.5 Return loss plot: ● 1st iteration ● 2nd iteration.

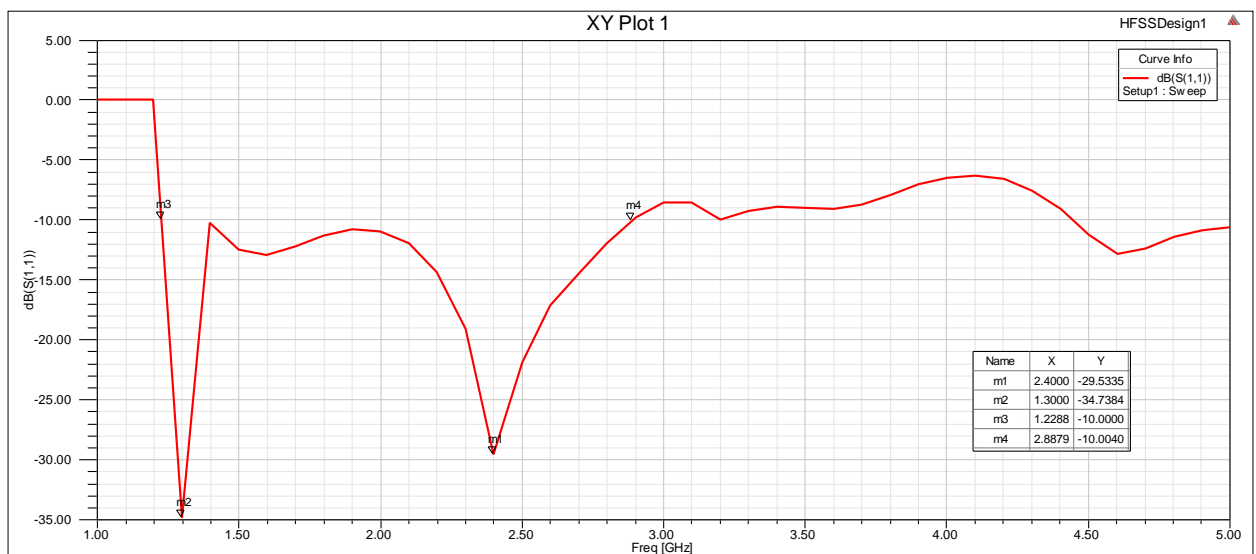


Figure 4.6 Return loss plot for 3rd iteration.

From the graph values, the impedance bandwidth was calculated by the difference between 'higher cut-off frequency' and 'lower cut-off frequency'. Also, the 'center frequency' is calculated by taking an average of both frequency values. To calculate the fractional bandwidth, impedance bandwidth is divided by center frequency

Fractional Bandwidth of band (1.2-2.9) GHz =>

$$\text{Impedance Bandwidth} = f_H - f_L = 2.9 - 1.2 = 1.7 \text{ GHz}$$

$$\text{Center frequency} = \left(\frac{f_H + f_L}{2} \right) = \frac{1.2 + 2.9}{2} = 2.05 \text{ GHz}$$

$$\text{Fractional Bandwidth} = \left(\frac{f_H - f_L}{f_c} \right) \times 100\% = 82.93\% \text{ which is greater than } 50\%$$

The VSWR plot and the 3D polar plot are given in Figures 4.7 and 4.8, respectively. The radiation pattern in elevation and the azimuthal plane is shown in Figure 4.9. Three different frequency values have been taken, at maximum, First resonating frequency and second resonating frequency at $\phi = "0 \text{ degrees}"$ and $"90 \text{ degrees}."$ The red curve represents $"0 \text{ degrees}"$, and the violet curve represents $"90 \text{ degrees}."$

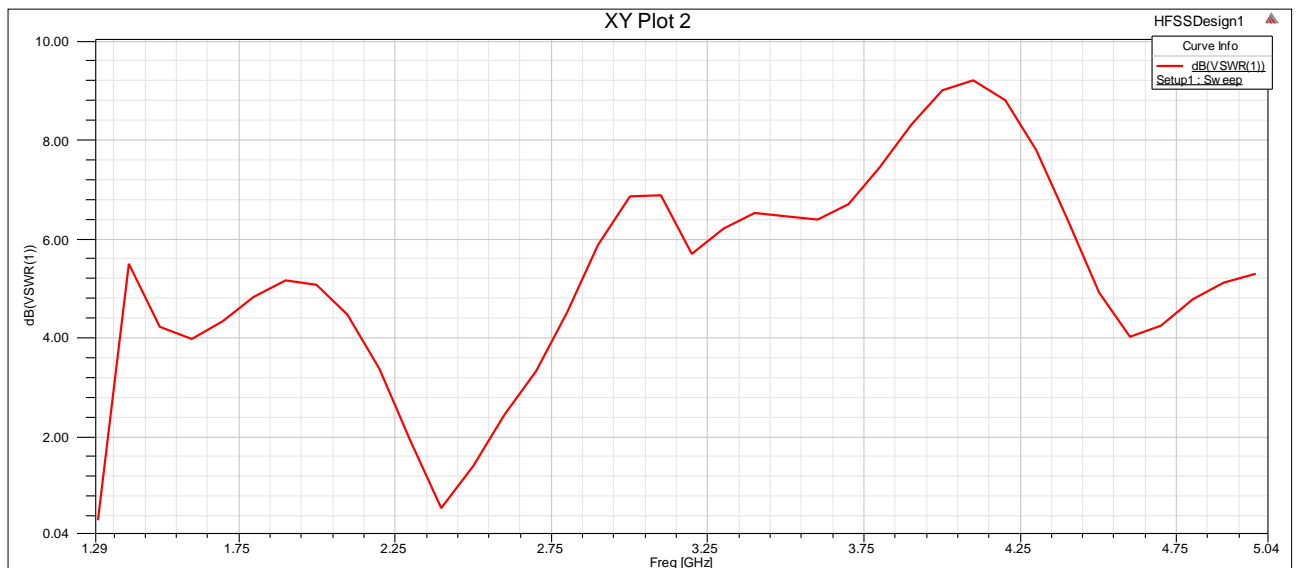


Figure 4.7 VSWR Plot for 3rd iteration.

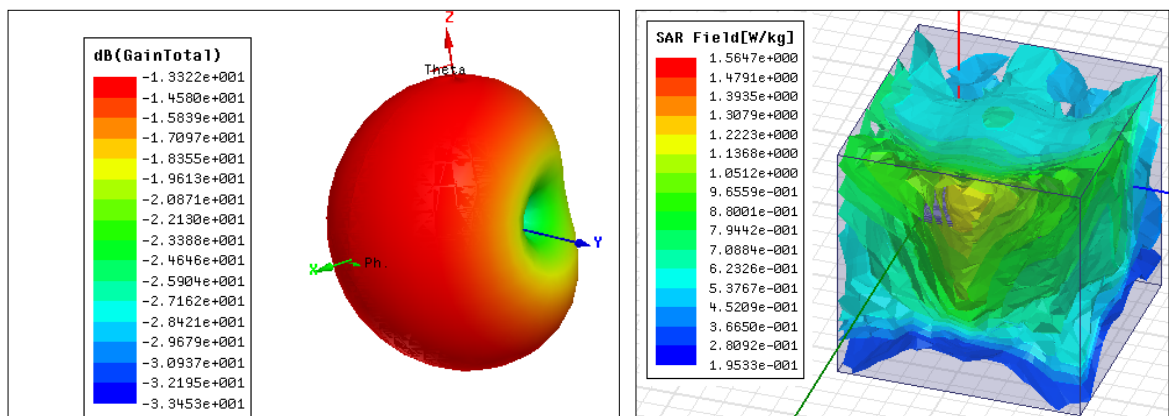


Figure 4.8 3-Dimensional polar plot and SAR plot.

SAR (specific absorption rate) when the input power was 1 Watt is 391.1 W/kg. All the new designs of wireless instruments shall realize the SAR values of 1.6 W/kg averaged over 1 gram of human tissue. On reducing the input power to 4mW, the SAR value is 1.56 W/kg which comes under the minimum allowed SAR value.

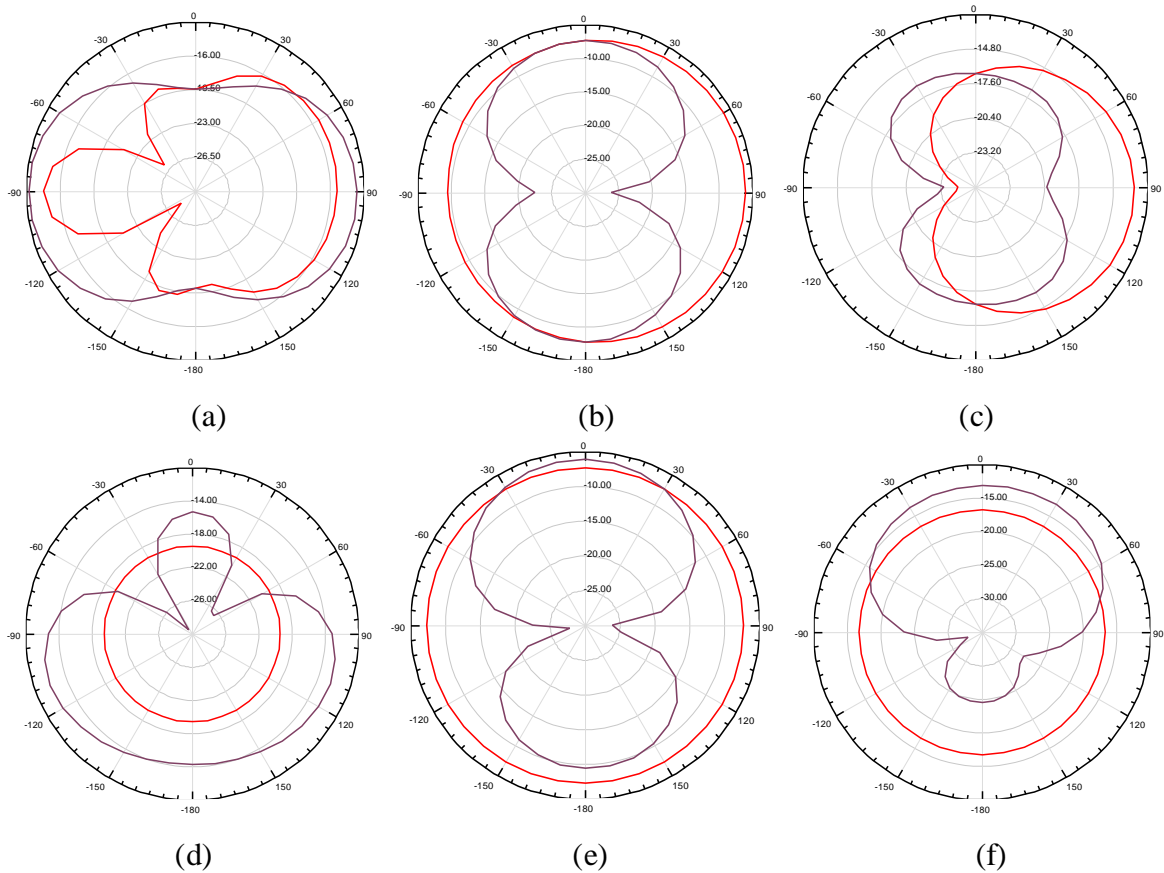


Figure 4.9 E-field distribution (a) at maximum frequency = 5 GHz (b) at first resonating frequency = 1.3 GHz (c) at second resonating frequency = 2.4 GHz.

H-field distribution (a) at maximum frequency = 5 GHz (b) at first resonating frequency = 1.3 GHz (c) at second resonating frequency = 2.4 GHz

4.4 PLACEMENT OF IMPLANTABLE ANTENNA INSIDE HUMAN BODY.

4.4.1 Inside the muscle layer.

The biomedical implantable antenna proposed earlier is now placed in the muscle layer with a dielectric coefficient (ϵ) of 52.79 and bulk conductivity (σ) of 1.705. The antenna is placed at different depths of the muscle layer, as shown in figure 4.10 and various parameters are analyzed and tabulated in Table 4.4

4.4.2 2-layer and 3-layer model.

The biomedical implantable antenna proposed earlier is now placed in the two-layer model, with the muscle layer having a dielectric coefficient (ϵ) of 52.79 and bulk conductivity (σ) as 1.705 and fat layer having dielectric coefficient (ϵ) as 5.285 and bulk conductivity (σ) as 0.102. This is the two-layer model [12]. One more layer of skin is added, having a dielectric coefficient (ϵ) of 42.92 and bulk conductivity (σ) of 1.562. The antenna is placed 6mm deep in the muscle layer, as shown in the figure and various parameters are analyzed and tabulated in Table 4.

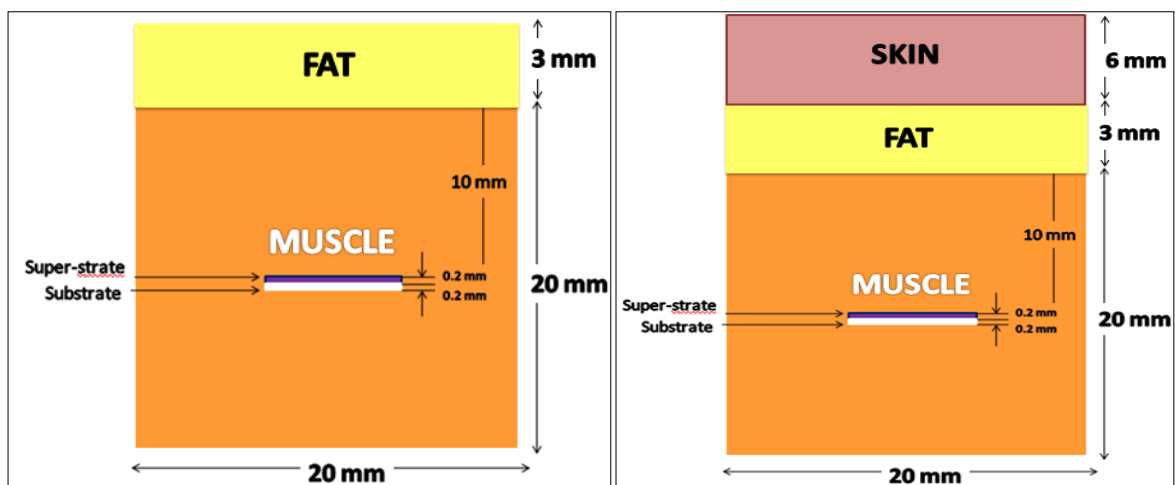


Figure 4.10 2-layer and 3-layer model

4.5 SIMULATION RESULTS

A. Return loss plot (S_{11} parameter)

The return loss plot for various values of depths inside the muscle layer is shown in figure 4.11 and inside two-layer (muscle, fat) and three-layer (muscle, fat, skin) in figure 4.10. From the graphs, the impedance bandwidth and the center frequency were calculated. From

these values , fractional bandwidth is also calculated. At the resonant frequency, return loss values are found and tabulated in Table 4.5

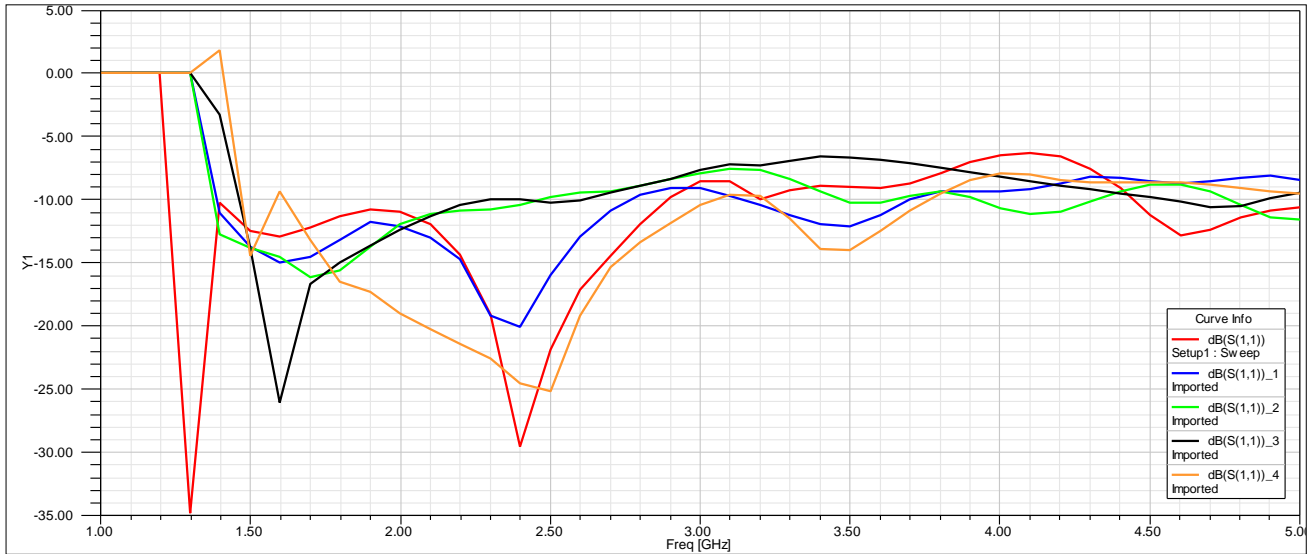


Figure 4.11 Return loss plot. ● 10mm ● 8mm ● 6mm ● 4mm ● 2mm

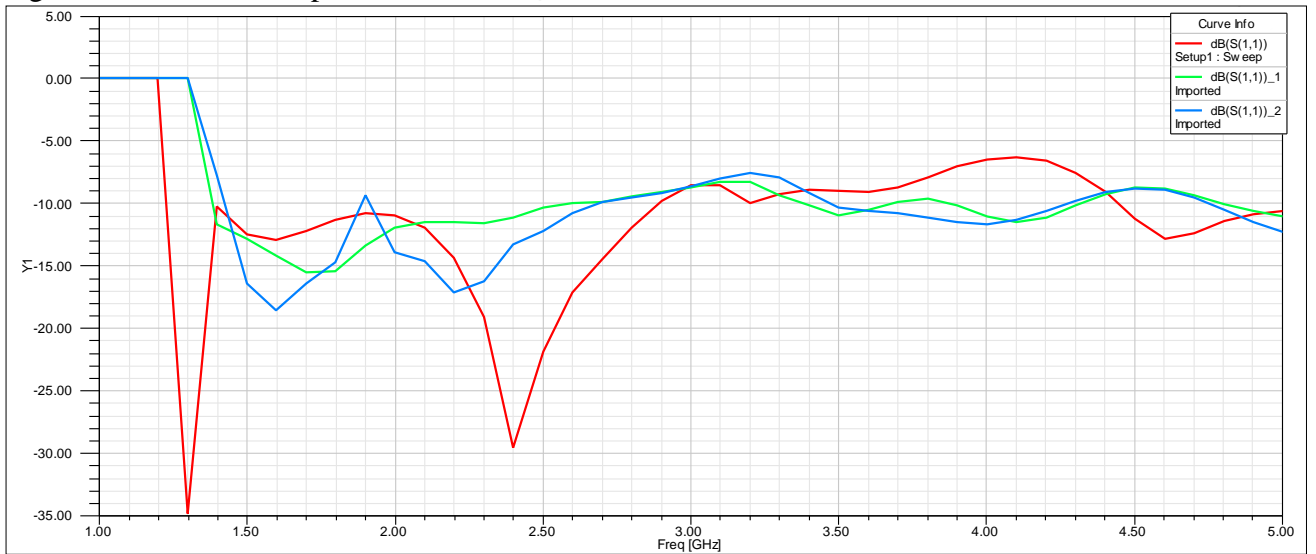


Figure 4.12 Return loss plot. ● 1-layer ● 2-layer ● 3-layer

4.6 SUMMARY

Results have been compared for different iterations on various parameters and is tabulated in Table 4.3. Our proposed antenna shows the best result of gain and dual-band characteristics.

PARAMETERS	ITERATION 1	ITERATION 2	ITERATION 3
Gain (dB)	-13.4	-13.3	-13.4
Return loss (dB)	-32.67	-26.7	(i) -34.7 (ii) -29.5
Fractional Bandwidth	27.45%	60.46%	82.93%
Frequency Band	(2.2-2.9) GHz ISM band	(1.5-2.8) GHz ISM band	(1.2-2.9) GHz WMTS, ISM band
SAR at power = 1 Watt	405.2	404.1	410.9

Table 4.3 Comparison of different iterations on the basis of various parameters.

- From the table, we can infer that fractional bandwidth has significantly improved with the increase in the number of iterations. The final antenna shows ultra-wideband characteristics that can work for two different medical bands: ISM (Industrial, scientific and medical) and WMTS (Wireless Medical Telemetry Service). Also, not much change is observed in gain, SAR, and return loss values.

PARAMETERS	Depth inside the muscle layer				
	10mm	8mm	6mm	4mm	2mm
Gain (dB)	-13.3	-12.5	-11.3	-13.9	-13.5
Return loss (dB)	(i) -34.7 (ii) -29.5	(i) -20.02 (ii) -14.92	-16.1	-26.04	-25.11
Fractional Bandwidth	82.93 %	66.35%	56.25%	44.68%	61.5%
Frequency Band	(1.2-2.9) GHz WMTS, ISM band	(1.4-2.7) GHz WMTS, ISM band	(1.38-2.46) GHz WMTS, ISM band	(1.46-2.3) GHz WMTS	(1.6-.04) GHz ISM
SAR at power = 1 Watt	410.9	391.17	393.8	421.1	440.06

Table 4.4 Various Antenna parameters when the antenna is placed at various depths of muscle layer.

- From the table, we can infer that the Gain and SAR are improved as the depth is decreased from 10mm to 6mm, but it starts degrading from 6mm to 2mm. Return loss and fractional bandwidth is reduced as the depth goes lower from 10mm to 4mm and then increased at 2 mm.

PARAMETERS	1-layer (muscle)	2-layer (muscle, fat)	3-layer (muscle, fat, skin)
Gain (dB)	-13.3	-10.9	-10.5
Return loss (dB)	(i) -34.7 (ii) -29.5	-15.4	(i) -18.5 (ii) -17.07
Fractional Bandwidth	82.93%	60.65%	60.82 %
Frequency Band	(1.2-2.9) GHz WMTS, ISM band	(1.4-2.6) GHz WMTS, ISM band	(1.43-2.68) GHz ISM band
SAR at power = 1 Watt	410.9	391.4	354.6

Table.4.5 Various Antenna parameters when the antenna is placed in different layers models.

From the table, we can infer that the gain and SAR are improved as the number of layers increases, but the return loss and fractional bandwidth are reduced

CHAPTER-5

GAIN ENHANCEMENT OF
BIOMEDICAL
IMPLANTABLE ANTENNA

5.1 INTRODUCTION

Implantable antennas have some limitations, including miniaturization of the antenna and low SAR values up to a specified limit, along with biocompatibility of the antenna to ensure the patient's safety. Given below are some factors affecting the design of the implantable antenna[10].

5.1.1 Radio wave propagation inside a human body.

Human body provides a lossy environment to the radio waves and absorbs them making the propagation complex as compared to free space.

Equation of an EM wave travelling in Z-direction is given by-

$$E(z) = Ee^{-\gamma z} \quad (5.1)$$

where E= amplitude of wave , γ = propagation constant.

As the value of γ increases, attenuation of wave travelling in inhomogenous region also increases. The value of complex propagation constant depends upon permittivity, permeability and conductivity of the medium.

$$\gamma = j\omega \sqrt{\mu\epsilon} \quad (5.2)$$

where $\mu = \mu_x \mu_0$, "permeability of the medium" and $\mu = \mu_0$ for "human tissues."

The permittivity of the lossy medium is given by equation.

$$\begin{aligned} \epsilon(\omega) &= \epsilon'(\omega) - j \epsilon''(\omega) \\ &= \epsilon_r'(\omega)\epsilon - j \epsilon_r''(\omega) \epsilon_0 \end{aligned} \quad (5.3)$$

where the real part of relative permittivity is defined by ϵ' and the imaginary part is by ϵ'' .

$$\text{where, } \epsilon_r''(\omega) = \frac{\sigma}{\omega \epsilon_0} \quad (5.4)$$

$$\tan\theta = \frac{\epsilon_r''}{\epsilon_r'} \quad (5.5)$$

where, σ = conductivity of the medium and $\tan\theta$ is loss tangent.

- With the increase in conductivity, complex permittivity and loss tangent increases making the medium lossy. Conductivity is maximum in case of muscle, then skin, and then fat layers.

5.1.2 EM wave propagation speed inside the human body.

The speed of wave depends on permittivity and conductivity of the medium and is reduced when travels inside the human body [10]. The propagation speed consists of phase velocity (V_p) and group velocity (V_g).

$$V_p = \frac{\omega}{\beta} \quad (5.6)$$

$$V_g = \frac{\partial \omega}{\partial \beta} \quad (5.7)$$

where ω is the angular frequency and β is the phase constant.

Speed depends on the phase constant and thus decreases when conductivity increases.

5.1.3 Effective wavelength

Wavelength is given by the formula,

$$\lambda = \frac{2\pi}{\beta} \quad (5.8)$$

phase constant (β) is directly proportional to conductivity and is inversely proportional to wavelength. Hence, when the conductivity increases, wavelength decreases making the size of the antenna smaller.

5.2 GAIN ENHANCEMENT TECHNIQUES

As we have seen, many factors affect the performance of the implantable antenna, and the gain we have received is deficient. So, to increase it, we have applied some techniques given below.

5.2.1 Encapsulation coating around the antenna.

From table 4.3, we can infer that the final iteration of the fractal antenna had a gain of -13.4 dB. To improve this, a thin layer of Teflon with a dielectric constant of 2.08 and thickness 0.1 mm is coated around the antenna, as shown in figure 5.1. 3-D polar plot after encapsulation is shown in Figure 5.4 (b). [14]

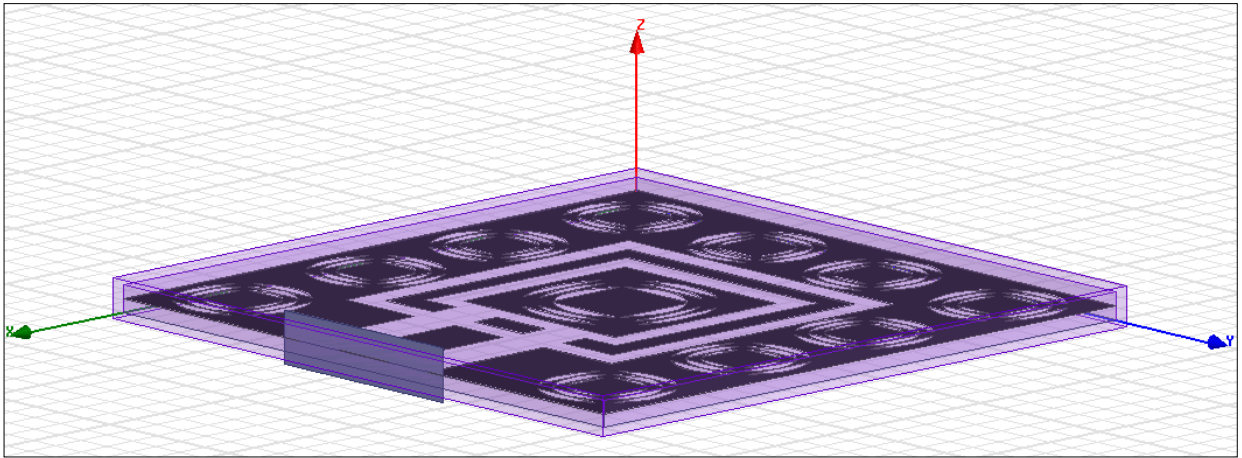


Figure 5.1 Encapsulation layer of teflon around the implantable antenna.

5.2.2 External parasitic ring

By coupling the exiting electromagnetic wave to an external parasitic ring, antenna performance can be improved. This ring is placed on the muscle layer with a radius of 24mm and thickness of 3 mm, as shown in figure 5.2. The 3-D polar plot is shown in Figure 5.4 (c).

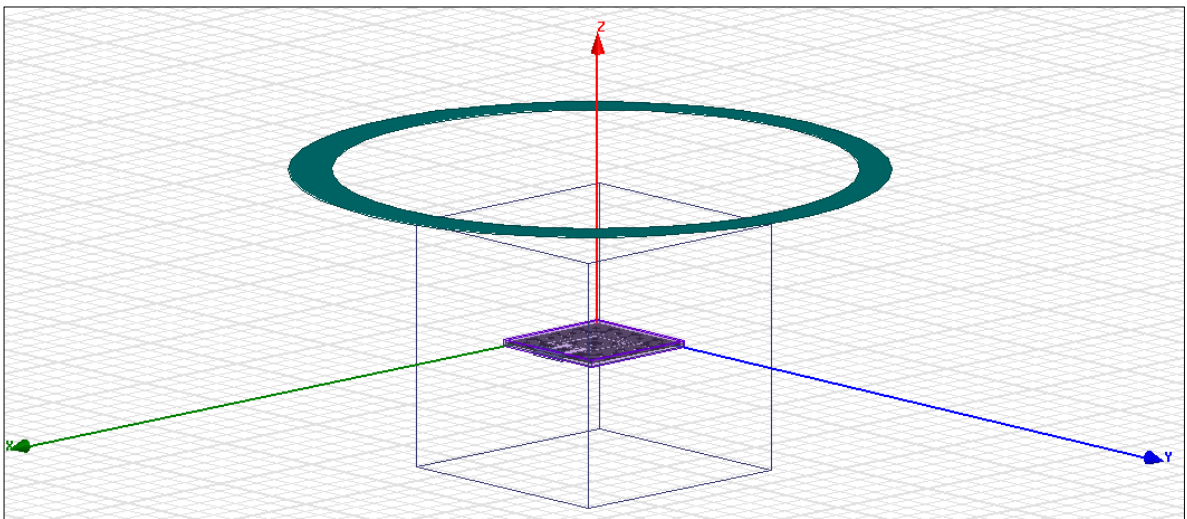


Figure 5.2 External Parasitic ring structure of radius 24 mm and thickness 3 mm.

The radius and width of the ring have been optimized to get the best results for antenna gain and tabulated in Table 5.1. The best antenna gain results are when the radius of the ring is 24mm and the width 3mm.

S. No.	Radius (mm)	Gain (dB)
1.	20	-10.8
2.	21	-7.84
3.	22	-6.69
4.	23	-5.88
5.	24	-5.83
6.	25	-5.9
7.	26	-6.53

S. No.	Width (mm)	Gain (dB)
1.	0.5	-6.62
2.	1	-6.55
3.	1.5	-6.13
4.	2	-6.06
5.	2.5	-5.95
6.	3	-5.83
7.	3.5	-5.95

Table 5.1 Optimizing radius and width of the ring.

5.2.3. External parasitic lens

An external hemispherical lens was designed and investigated to be placed on the muscle layer over the implanted antenna to improve the implanted antenna performance, as shown in figure 5.3. It was made up of pyrex material with a dielectric constant of 4.82. To minimize the spreading of incident divergent energy in undesired directions, Lens antennas are used. They collimate incident energy-producing highly directive beams by converting divergent energy waves to plane waves [12]. The 3-D polar plot is shown in Figure 5.4 (d).

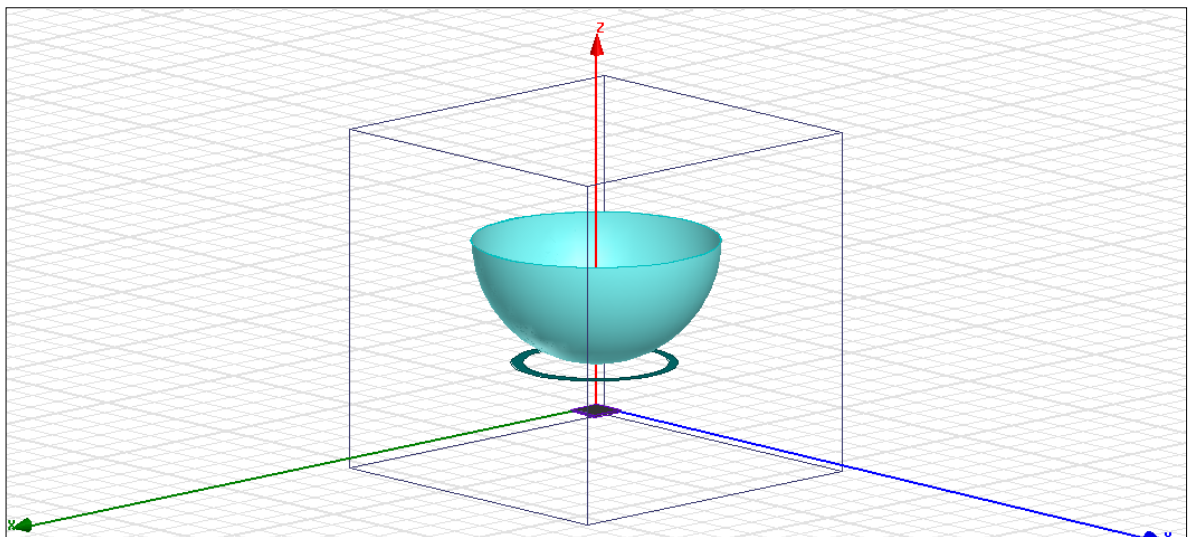


Figure 5.3 External Parasitic lens structure of radius 32 mm and thickness 0.1 mm

The lens radius has been optimized to get the best results for antenna gain, as shown in Table 5.2. The best antenna gain results are when the lens radius is 32 mm and the width 0.1mm.

S. No.	Radius (mm)	Gain (dB)
1.	28	-4.55
2.	32	-4.53
3.	34	-4.55
4.	36	-4.6
5.	38	-4.67
6.	40	-4.69

Table 5.2 Optimizing radius of the lens of the implantable antenna.

5.3 Simulation Results

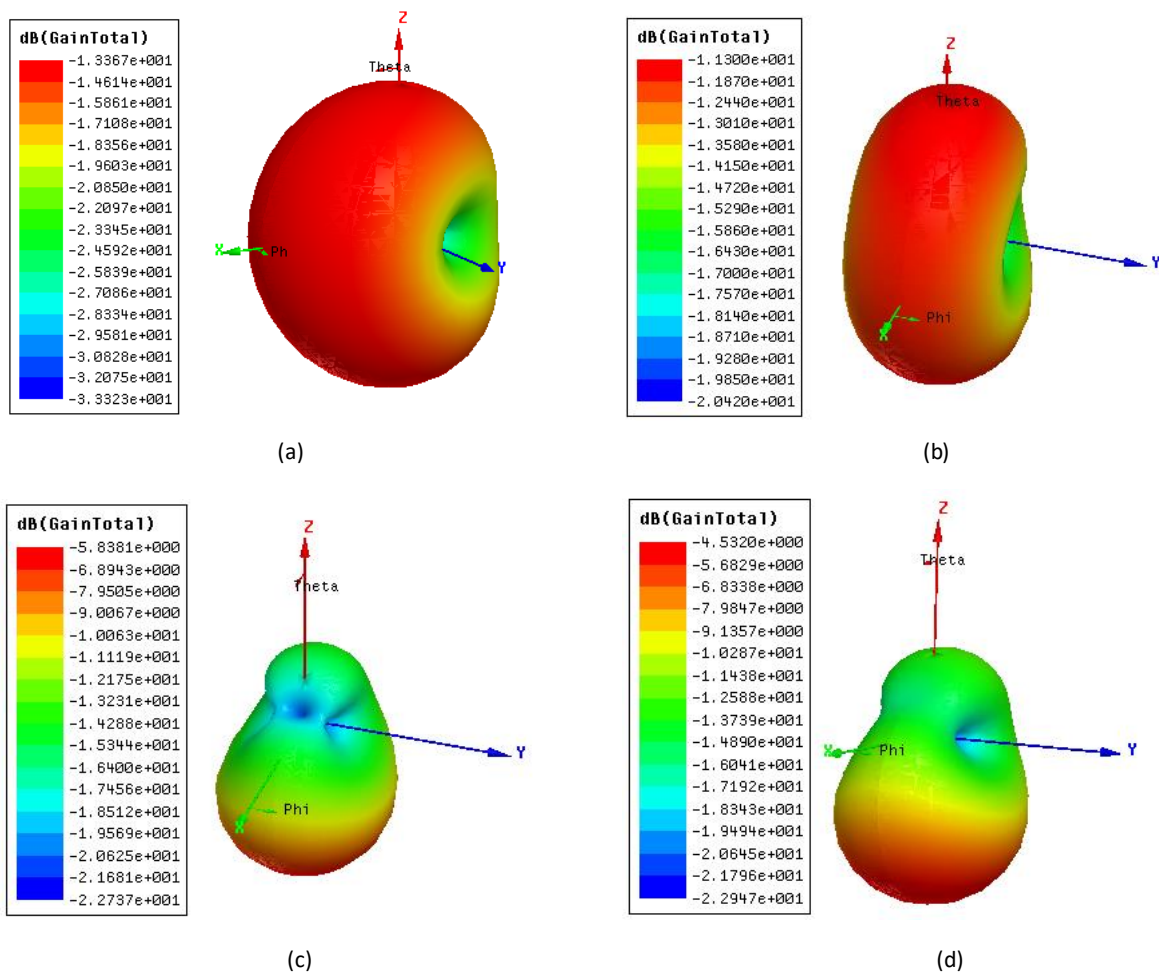


Figure 5.4 3-Dimensional polar plot showing gain of the antenna with various gain enhancement techniques used. (a) Third iteration fractal antenna (b) After encapsulation c) With external parasitic ring. (d) With hemispherical lens.

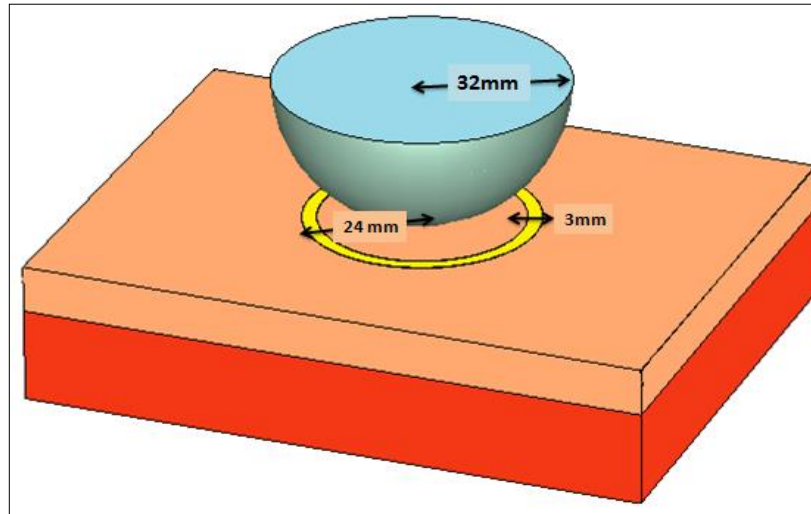


Figure 5.5 Implantable antenna with external parasitic ring and lens.

After using all the gain enhancement techniques together in the final iteration of the fractal antenna, a total of 8.8 dB of gain has been improved, as shown in figure 5.5. The return loss plot for all the three techniques is combined and shown in the figure. Return loss plot, SAR, and 2-D radiation patterns of the final antenna with all the three techniques together has been shown in Figure 5.6, 5.8, and 5.9, respectively. The return loss plot for the final antenna is shown in Figure 5.7.

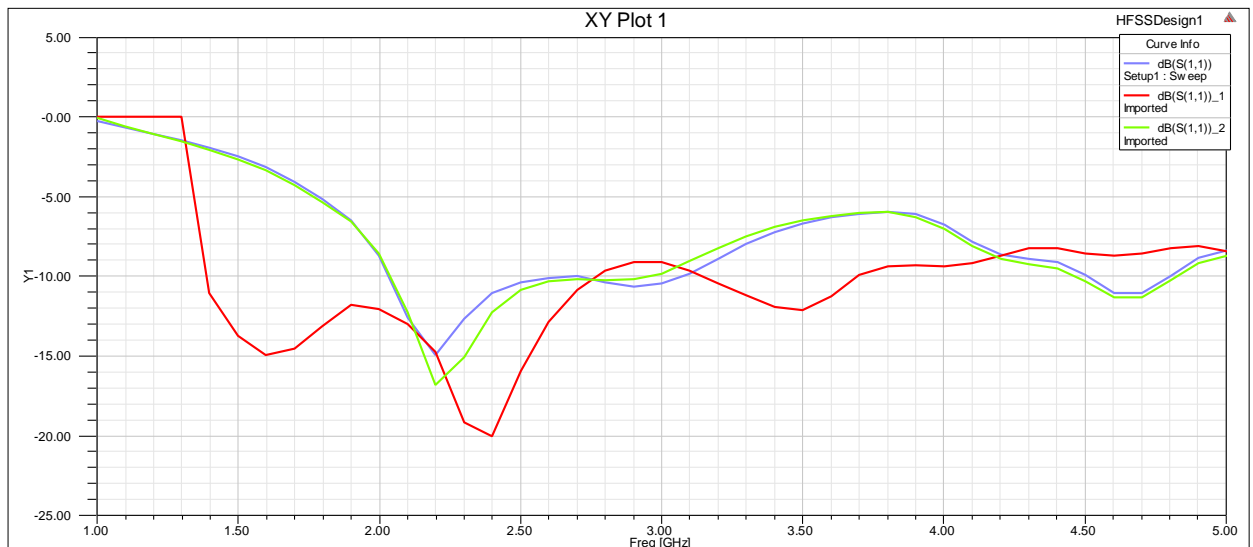


Figure 5.6 Return loss plot. ● Final (3rd) iteration ● after encapsulation layer ● after ring.

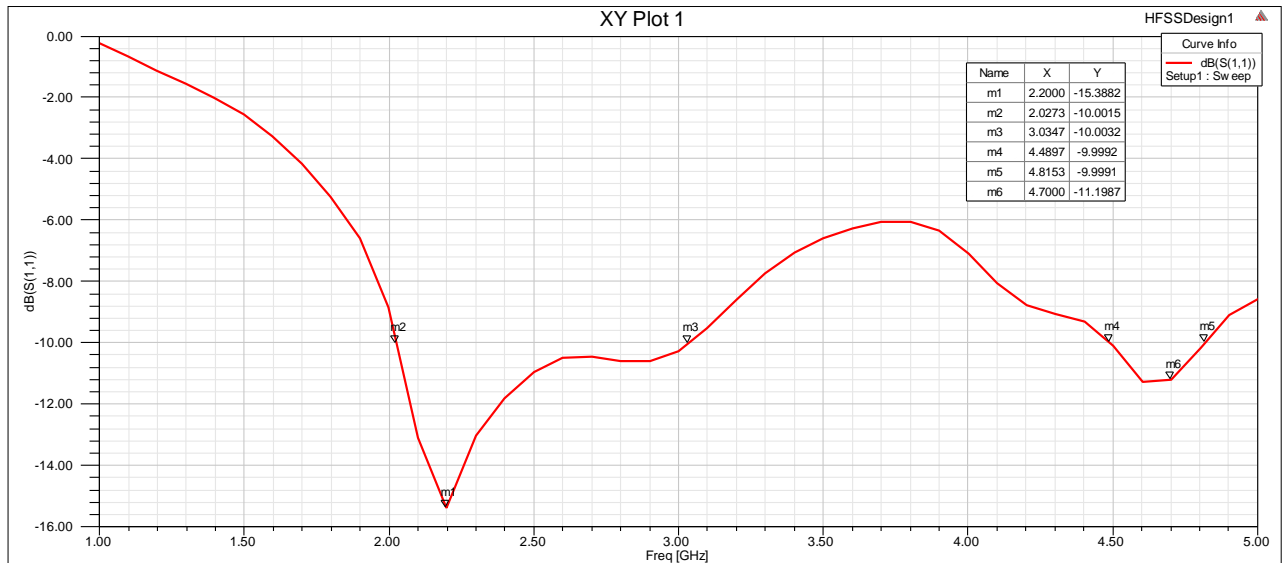


Fig.5.7 Return loss plot (S11 parameter) for all the techniques combined.

Observing the return loss plot, return loss was found to be -15.38 dB at the first resonating frequency, 2.2 GHz, and - 11.2 dB at the second resonating frequency, 4.7 GHz. Impedance bandwidth of the first band (3-2 GHz) is 1 GHz and the second band (4.4-4.8 GHz) is 0.4 GHz. From these values, fractional bandwidth is calculated as 40 % (wideband) for the first band and 8.7 % for the second band.

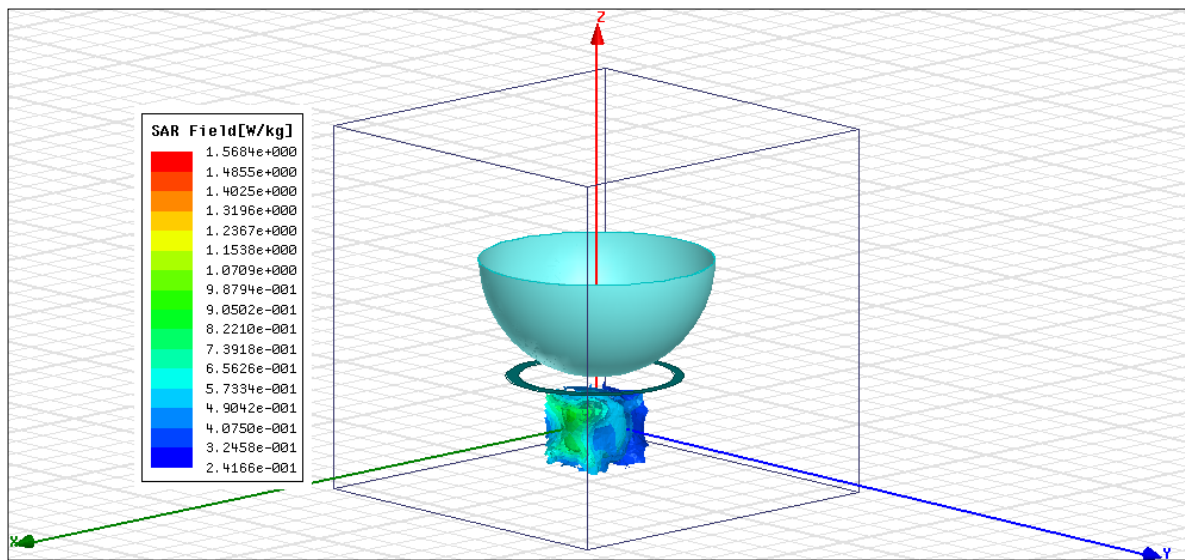


Figure 5.8 SAR (Specific absorption rate) plot

SAR (specific absorption rate) when the input power was 1 Watt is 364.74 W/kg. India has adopted the most strict international norms for wireless communication. All the new designs of wireless instruments shall realize the SAR values of 1.6 W/kg averaged over 1 gram of human tissue. On reducing the input power to 4.3 mW, the SAR value is 1.56 W/kg which comes under the minimum allowed SAR value. The far-field radiation pattern showing the E-plane and H-plane patterns at the operating frequency (2.45 GHz) and the resonating frequency (2.2 GHz) is shown in figure 5.9.

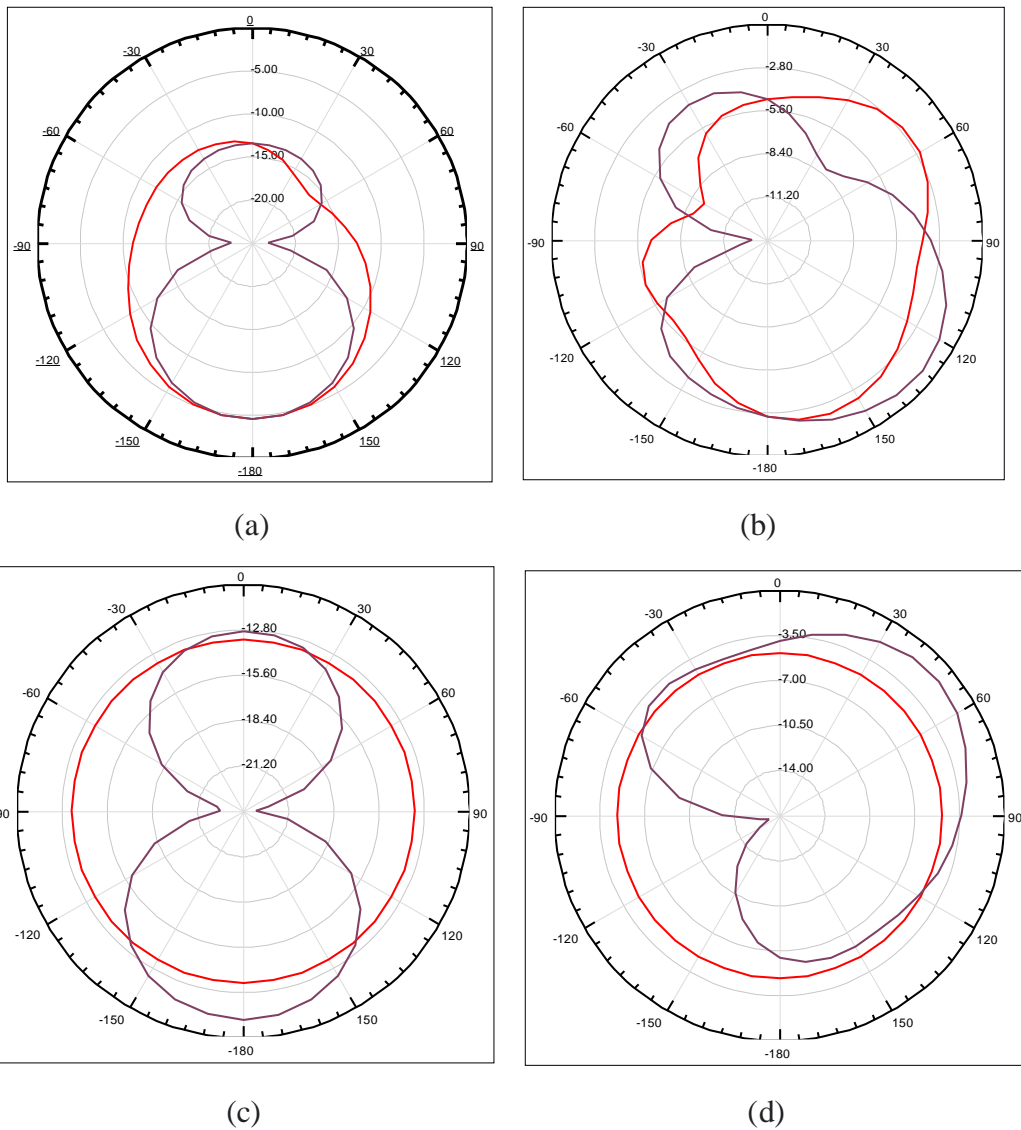


Figure 5.9 E-field distribution (a) at operating frequency = 2.45 GHz (b) at resonating frequency = 2.2 GHz.

H-field distribution (a) at operating frequency = 2.45 GHz (b) at resonating frequency = 2.2 GHz

5.4 SUMMARY

Due to the lossy environment created by human tissue, the gain was low. So, various gain enhancement techniques are used, namely encapsulation, external parasitic ring, and lens.

- ✓ A gain enhancement of 2.1 dB has been observed when an encapsulation layer made of Teflon is used around the antenna.
- ✓ Gain enhancement of 5.5 dB has been observed when an external parasitic ring has been used.
- ✓ Also, a Gain enhancement of 1.3 dB is observed when an external parasitic lens is used. Combining all the three techniques, an 8.9 dB gain has been improved.
- ✓ It has also been observed that due to the addition of these enhancement techniques, the SAR value of the antenna has been reduced by 26.36 W/kg.

CHAPTER-6

CONCLUSION AND FUTURE WORK

1.1 CONCLUSION

This thesis has been an effort to understand and contribute to the antenna theory's combination with fractal geometry and its application in the biomedical field. The design aims to reduce the physical antenna size and increase the impedance bandwidth and gain. Fractal antenna design and gain enhancement techniques are presented in this thesis.

Three antenna structures using Sierpinski Gasket, Sierpinski Carpet, and Koch curve structures to make the antenna suitable for multiband applications. Additionally, the ground is defected in the shape of a semi- ellipse to enhance the bandwidth, and further size is reduced. Material polyester ($\epsilon = 3.2$) has been chosen to design the proposed antenna for wearable antenna applications, and the substrate thickness is 1mm. The microstrip feed technique is used as it provides improved results. Table 6.1 below shows the comparison between different structures with different parameters.

PARAMETERS	REFERENCE [1]	SIERPINSKI GASKET GEOMETRY [ANTENNA 1]	SIERPINSKI CARPET GEOMETRY [ANTENNA 2]	KOCH CURVE GEOMETRY [ANTENNA 3]
GAIN	5.2115	5.5683	5.57	5.319
IMPEDANCE BANDWIDTH	(i) 6.2684	(i) 6.8167	(i) 1.16	6.45
	(ii) 8.2493	(ii) 12.6213	(ii) 3.7	7.28
			(iii) 11.92	
FRACTIONAL BANDWIDTH	(i) 81.04%	90.703 %	(i) 19.96 %	82.113 %
	(ii) 32.89%	46.663 %	(ii) 39.15 %	29.797 %
			(iii) 47.71 %	
RETURN LOSS (dB)	(i) -27.975	-28.9176	(i) -26.536	-31.6853
	(ii) -30.142	-27.643	(ii) -18.1865	-54.2024
			(iii) -34.7505	
RADIATION EFFICIENCY	97.11 %	98.42 %	94.15 %	98.114 %
FREQUENCY BANDS	(4-11) GHz	(4-11) GHz	(5-6) GHz	(4-11) GHz
	(21-29) GHz	(20-33) GHz	(7-11) GHz (19-31) GHz	(20-28) GHz

FREQUENCY BAND	C & X bands	C & X bands	C band	C & X band
	K band	K &Ka bands	X band K &Ka band	K band
RESONANT FREQUENCY	7.1 GHz	7.05 GHz	5.97 GHz	7.18 GHz
	22.8 GHz	23.59 GHz	8.8 GHz 21.17 GHz	25.47 GHz

Table 6.1 Comparison of different antennas proposed in this thesis and previous works based on various parameters.

The design and analysis of a biomedical implantable antenna are addressed in this thesis. With the help of the fractal geometry, the antenna is miniaturized and shows wideband characteristics as per the requirement for the implantable antenna. The materials for substrate and superstrate are assigned, keeping in mind the flexibility and biocompatibility of the antenna. Due to the lossy environment created by human tissue, the gain was low. So, various gain enhancement techniques are used, namely encapsulation, external parasitic ring, and lens [12]. A gain enhancement of 8.9 dB has been observed combining all the three techniques. It has also been observed that due to the addition of these enhancement techniques, the SAR value of the antenna has been improved. Table 6.2 below shows the comparison between different structures with different parameters

Parameters	Iteration 3	With encapsulation layer	With external parasitic ring	With external parasitic lens
Gain (dB)	-13.4	-11.3	-5.83	-4.53
Return loss (dB)	(i) -34.7 (ii) -29.5	-16.81	-14.91	-15.38
Fractional Bandwidth	82.93%	36.47 %	40.7 %	40%
Frequency Bands	(1.2-2.9) GHz WMTS, ISM band	(2.04-2.95) GHz ISM band	(2.03-3.07) GHz ISM band	(2.02-3.03) GHz ISM band
SAR at power 1 Watt	410.9	385.7	366.7	364.74

Table 6.2 Comparison of different antenna models proposed in this thesis for improved gain

1.2 FUTURE WORK

1. Different materials can be replaced for substrate according to various applications and then the performance can be analyzed.
2. More complex designed fractal antenna can be implemented for better Results and enabled for more than just two frequency bands.
3. Multi-band Fractal antenna for RF energy harvesting.
4. Reconfigurable Fractal Antenna can be designed for wireless communication.
5. Use of metamaterials to enhance Gain of the Fractal Antenna.

CHAPTER-7

REFERENCES

- [1]. M. Ramya and R. Rani, "A Compendious Review on Fractal Antenna Geometries in Wireless Communication", Proceedings of the Fifth International Conference on Inventive Computation Technologies (ICICT-2020)IEEE Xplore Part Number:CFP20F70-ART; ISBN:978-1-7281-4685-0
- [2]. S. Bhatia and J. Sivia, "A Novel Design of Wearable Fractal Antenna for Wideband Applications", International Conference on Advances in Human Machine Interaction (HMI - 2016), March 03-05, 2016, R. L. Jalappa Institute of Technology, Doddaballapur, Bangalore, India
- [3]. A. Tripathi, P. Rao and R. Mishra, "An AMC Inspired Wearable UWB Antenna for Skin Cancer Detection", 2020 International Conference on Electrical and Electronics Engineering (ICE3-2020)
- [4]. S. Joseph, B. Paul, S. Mridula and P. Mohanan, "CPW-Fed Fractal Antenna with Improved UWB Response", 2015 IEEE 4th Asia-Pacific Conference on Antennas and Propagation (APCAP).
- [5]. A. Mersani, L. Osman, J. Ribero, "Flexible UWB AMC Antenna for Early Stage Skin Cancer Identification," Progress In Electromagnetics Research M, Vol.80,71-81,2019.
- [6]. M. Jena, G. Mishra, A. Sahoo and B. Mangaraj. "Fractal Geometry and Its Application to Antenna Designs", International Journal of Engineering and Advanced Technology (IJEAT) ISSN: 2249 – 8958, Volume-9 Issue-1, October 2019.
- [7]. R. Kumar et al, "Hexagonal Shaped Body Wearable Textile Antenna on EBG Substrate Material," International journal of Computer Science and Mobile Computing, Vol.5 Issue.6, pp. 260-266, June-2016.
- [8]. A. Baroni, H. Rogier and P. Nepa, "Wearable Active Sierpinski Fractal Antenna for Off-Body Communication", APS 2015, Vancouver, Canada.
- [9]. A. Sharif, J. Ouyang, H. Chattha, M. Imran and Q. Abasi, "Wearable UHF RFID Tag Antenna Design using Hilbert Fractal Structure", 978-1-7281-2797-2/19/\$31.00 ©2019 IEEE.

- [10] M. Soliman and M. Chowdhury," Review on Medical Implantable Antenna Technology and Imminent Research Challenges " proceedings of the fifth international conference on initiative computation technologies (ICICT-2020) IEEE Xplore Part Number: CFP20F70-ART; ISBN:978-1-7281-4685-0.
- [11] S. Das and D. Mitra, "A compact wideband flexible implantable slot antenna design with enhanced gain" IEEE Transactions on Antennas and Propagation (Volume: 66, Issue: 8, Aug. 2018) DOI- 10.1109/TAP.2018.2836463, INSPEC Accession Number: 18006005.
- [12] S.Alamri, “ Implanted Antennas for Biomedical Applications ”, December 2016 / Department of Electrical and Electronics Engineering.
- [13] Francesco," Implantable Antennas for Biomedical Applications "December 2011/ Department of Electrical and Electronics Engineering.
- [14] K. Psathas, A. kiourti and K. Nikita," Biocompatibility of Implantable Antennas: Design and Performance Considerations ", The 8th European Conference on Antennas and Propagation (EuCAP 2014).
- [15] S. Suganthi, S. Raghavan, D. Kumar, J. Selvi, " Study of Compact Hilbert Curve Fractal Antennas for Implantable Medical Applications ", International Journal of Emerging Technology and Advanced Engineering (ISSN 2250-2459, Volume 2, Issue 10, October 2012)
- [16] S. Chen and C. Yang, " Implantable Fractal Dental Antennas for Low Invasive Biomedical Devices ", 978-1-4244-4968-2/10/\$25.00 ©2010 IEEE .
- [17] H. Liu and X. Liu, "A miniaturized differentially fed implantable hilbert curve fractal antenna at MICS band",
- [18] T. Das and S. Behera, " Design of a Compact antenna for Biomedical Applications ", Department of electronics and communication department, NIT Rourkela.
- [19] A. Bhattacharjee, A. S. Chowdhuri, A. Saha, A. Karmakar, D. Bhattacharya, "Compact fractal shaped mimo antenna for portable uwb applications ", in: 2020 IEEE Region 10 Symposium (TENSymp), 2020, pp.1600–1603.

CHAPTER - 8

PUBLICATIONS DETAILS

PAPER 1

Design and analysis of Multiband Fractal Antenna for UWB Communication

Nancy
Department of Electronics and
Communication engineering
Delhi Technological University
New Delhi, India
nancy_2k20moe04@dtu.ac.in

Kaushtabh Ranjan Singh
Department of Electronics and
Communication engineering
Delhi Technological University
New Delhi, India
kaushtabh@dtu.ac.in

Abstract— The paper aims at presenting the implementation and analysis of Fractal antenna by using different fractal geometries namely Sierpinski Gasket and Sierpinski Carpet, to improve the gain of the antenna along with the multiband characteristics for Ultra Wide Band (UWB) Communications. Fractals are utilized in improving several aspects of the antenna performance. Polyester as the substrate of the antenna has been used which makes it useful for Military applications. Different fractal geometries with their dimensions that have been later used in the designing part of the antenna and different antenna properties have been described. The antenna design along with the parametric study shows improvement in return loss plot, VSWR, Gain, Directivity, radiation, patterns and efficiency.

Keywords— Fractals, Fractal geometries, ultra-wideband, antenna, radiation pattern, gain.

I. INTRODUCTION

In today's modern world, the wireless communication industry has shown so much progress and growth following the initiation of the internet and cell phones. And thus, a need for more and more frequency bands. These devices also require antennas that are small, compatible, affordable, and operating for more than one operating frequency band while maintaining their performance. To overcome these challenges, a new scheme of multiband antennas is proposed.

Multiband antennas have various applications in modern wireless communication systems in which the downward and the roaming capability among multi-standards are demanded. The global system for mobile communication (GSM), the general packet radio service (GPRS), the wireless local area networks (WLAN), the universal mobile telecommunications system (UMTS), etc. are generally dual-band or multi-band wireless standards communication devices. So, both the requirement of the compact and multiband antenna is fulfilled by fractal antennas. These antennas utilize fractal geometry concepts that are the self-similar patterns to maximize the effective length of the

antenna using Fractal geometry [2]. The contribution in this paper is as follows:

- The multi-band aspect of microstrip antenna is explored with special emphasis on its design based on Sierpinski gasket fractal geometry resulting in its multi-band behavior.
- An antenna with polyester as substrate and with microstrip feed was designed mainly for military applications.
- Defected ground structure was used to improve impedance bandwidth. Multiple iterations were done in order to get a dual-band antenna with high bandwidth.

The paper is organized as follows: Section II gives the basic antenna design of the proposed antenna. Following this is Section III presenting the simulation results which validate the accuracy of the analysis and demonstrates the performance improvement with the proposed strategy. Finally, Section IV concludes this paper.

II. FRACTAL GEOMETRY

The main concept behind the fractal antenna was to increase the perimeter or the length of the conductor within a restricted given area or volume, that receives or radiates the electromagnetic radiations. To implement this, self-similar structures were used to design an antenna. They are also known as space-filling curves. The different iterations in a design can produce different size geometries that have different electrical length and thus resonates at different frequencies which also make these antennas wideband or even multiband [1]. Fractal design has commonly two dimensions and components:

A) The Initiator (0th stage) which is the basic structure of the fractal geometry.

B) The Generator which is the structure which is repeated in a sequential pattern on the initiator in the consequent stages with the different dimensions as shown in Figure.1

Formula for self-similarity dimension is given as:

$$D_s = \log(N) / \log(1/s) \quad (1)$$

Where, 's' is the scaling factor and 'N' is the number of self-similar copies.

PAPER 2

Biomedical Implantable Antenna with Fractal Geometry

Nancy
Department of Electronics and
Communication engineering
Delhi Technological University
New Delhi, India
nancy_2k20moe04@dtu.ac.in

Kanabath Rangan Singh
Department of Electronics and
Communication engineering
Delhi Technological University
New Delhi, India
kanabath@dtu.ac.in

Abstract— This paper aims at presenting the design and implementation of the fractal antenna with a dual-ring slot structure for biomedical applications in the ISM frequency band (2.4 GHz - 2.48 GHz). Inscribed square circular fractal geometry is used to make the antenna compact and with wideband characteristics. Thin and biocompatible substrate-superstrate layers are used in designing this implantable antenna to attain human body insulation and flexibility. The human body proves to be a hostile environment from radio wave propagation in contrast with the conventional wireless system. This environment is extremely lossy and affects the antenna parameters and hence lowers the gain of the implantable antenna. To minimize this effect, techniques like encapsulation are used. Moreover, a ring and a hemispherical lens is used externally in order to enhance the gain and reduce SAR. A comparative analysis has been done for the various stages of the designed antenna to get the best one suitable for the application.

Keywords: Fractals, Fractal geometries, biomedical applications, Gain enhancement, wideband.

I. INTRODUCTION

Wireless medical applications have made a tremendous growth in the healthcare sector over the past decade. Implantable antennas are used in heart pacemakers, retinal prosthesis and even in endoscopy in case of ulcers, cancerous tumours, inflammatory bowels etc. This technology is of great use in continuously monitoring the patient that will reduce the risk of complications. This can also be cost effective as the patient need not to be admitted in hospital in some cases. With antenna implanted in the body one can continuously monitors patients's glucose level, blood pressure, pulse rate etc and this vital information is transmitted to external devices via a wireless communication link [8].

Biomedical implantable antenna requires some basic properties like compact size, low specific absorption rate, flexible and with wideband characteristics. For proper positioning of the antenna inside the human body, the size of the antenna must be small. Various techniques are used for miniaturization of antenna including concentric ring slots in the shape of rectangle making the antenna compact and simple. Two resonant frequencies that are nearly spaced are excited by this dual ring topology that results in larger bandwidth [2]. Along with this, fractals is also used that are the self-similar patterns to maximize the effective length of the antenna which makes the antenna multiband, wideband, and also miniaturized without any use of inductors or capacitors. They are also known as space-filling curves as we can increase the perimeter while keeping its area constant. Many different fractal geometries like Sierpinski

gasket, Sierpinski carpet, Koch curve, Minkowski island, etc. are used which first involves a basic shape that is repeated over and over with every iteration making it a multiband antenna [1].

Flexibility is another requirement for the implantable antenna. This prevents the breakage of the antenna with any movement of the body part or the muscle. Thin and flexible layers of substrate and superstrate are used to provide flexibility. Also, these layers should be biocompatible [4] [5]. The Antenna is covered with a thin layer of biocompatible material to enhance its performance by reducing the absorption in the lossy environment. A reduced antenna gain has been observed due to the absorbing nature of the human body. So, to improve the antenna gain, different techniques are used namely external parasitic ring and hemispherical lens along with the encapsulation layer around the antenna [2].

II. FRACTAL GEOMETRY

The main concept behind the fractal antenna was to increase the perimeter or the length of the conductor within a restricted given area or volume, that receives or radiates the electromagnetic radiations. To implement this, self-similar structures were used to design an antenna. They are also known as space-filling curves. The different iterations in a design can produce different size geometries that have different electrical length and thus resonates at different frequencies which also make these antennas wideband or even multiband [1]. Fractal design has commonly two dimensions and components:

A) The Initiator (0th stage) which is the basic structure of the fractal geometry.

B) The Generator which is the structure which is repeated in a sequential pattern on the initiator in the consequent stages with the different dimensions as shown in Figure.1

Formula for self-similarity dimension is given as:

$$D_s = \frac{\log(N)}{\log(1/s)} \quad (1)$$

Where, 's' is the scaling factor and 'N' is the number of self-similar copies.

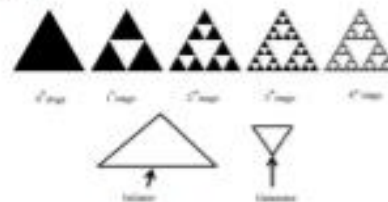


Fig.1 Sierpinski Gasket Fractal Geometry

SIMILARITY INDEX 18% VERIFIED

Thesis

ORIGINALITY REPORT

18%

SIMILARITY INDEX

13%

INTERNET SOURCES

12%

PUBLICATIONS

9%

STUDENT PAPERS

PRIMARY SOURCES

1	Submitted to Delhi Technological University Student Paper	2%
2	ethesis.nitrkl.ac.in Internet Source	1%
3	Soumyadeep Das, Debasis Mitra. "A Compact Wideband Flexible Implantable Slot Antenna Design With Enhanced Gain", IEEE Transactions on Antennas and Propagation, 2018 Publication	1%
4	www.ijecse.org Internet Source	1%
5	archives.univ-biskra.dz Internet Source	<1%
6	www.iosrjournals.org Internet Source	<1%
7	R. Kumari, M. Kumar. "Design of Multiband Antennas for Wireless Communication", 2013 International Conference on Communication Systems and Network Technologies, 2013	<1%